Short-term synaptic plasticity at the mossy fiber synapse of the rodent hippocampus

Dissertation

zum Erlangen des Doktorgrades (Dr. rer. nat.)

der Mathematisch-Naturwissenschaftlichen Fakultät

der Rheinischen Friedrich-Wilhelms-Universität Bonn

vorgelegt von

Malte Merkens

aus Düren

Bonn, März 2009

Angefertigt mit Genehmigung der Mathematisch-Naturwissenschaftlichen Fakultät
der Rheinischen Friedrich-Wilhelms-Universität Bonn

Erstgutachter: Prof. Dr. Heinz Beck

Zweitgutachter: Prof. Dr. Horst Bleckmann

Fachnaher Gutachter: Prof. Dr. Christian Steinhäuser

Fachangrenzender Gutachter: Prof. Dr. Dieter O. Fürst

Hiermit versichere ich, dass ich die vorliegende Dissertation selbstständig und ohne Verwendung anderer als der angegebenen Quellen und Hilfsmittel angefertigt habe. Diese Arbeit hat bisher keiner anderen Prüfungskommission zur Begutachtung vorgelegen.

Malte Merkens Bonn, 1. März 2009

Danksagung

Zu allererst möchte ich mich bei Prof. Dr. H. Beck für die Möglichkeit bedanken, diese Dissertation in seiner Arbeitsgruppe anfertigen zu dürfen. Während dieser Zeit stand seine Tür bei Problemen stets offen für mich und ich konnte mich immer darauf verlassen, dass er mit Rat beiseite stand.
Prof. Dr. H. Bleckmann möchte ich besonders danken, weil er mein Interesse an der Elektrophysiologie geweckt hat und weil er sich bereit erklärt hat, als Gutachter zu fungieren.
Ein besonderer Dank gilt Dr. T. Opitz für die mühevolle Durchsicht des Manuskripts und die damit verbundenen hilfreichen Kommentare.
Ich möchte mich ebenso bei Prof. Dr. D. Dietrich bedanken, ohne dessen Hilfe die Entwicklung des mathematischen Modells in dieser Form wohl nicht möglich gewesen wäre.
Desweiteren möchte ich mich bei Dr. Steven Barnes und Dr. Britta Sommersberg bedanken, weil diese beiden es geschafft haben, mich während meiner langwierigen Versuche bei Laune zu halten.
Ebenso möchte ich mich für die langjährige Hilfsbereitschaft bei der gesamten Arbeitsgruppe Beck bedanken, durch die meine Zeit im Labor sehr angenehm wurde.
Besonderer Dank gilt meinen Freunden, die immer für mich da waren, und es immer geschafft haben mich wieder aufzubauen.
Ein spezieller Dank geht an Julia Welschoff, weil ich ohne sie wahrscheinlich immer noch beim Korrigieren wäre, und einfach weil es sie gibt.
Vor allem aber möchte ich meiner Familie danken, die es mir ermöglicht hat bis hierher zu kommen. Dafür, dass sie mich immer unterstützt hat, nie an mir gezweifelt hat und mir immer das Gefühl gegeben hat, dass Richtige zu tun.

Contents

Ein Zwerg, der auf den Schultern eines Riesen steht, kann weiter sehen als der Riese selbst.[1]

[1] Auf den Schultern von Riesen. Ein Leitfaden durch das Labyrinth der Gelehrsamkeit. 2. Auflage, 2004 von Robert K. Merton, Suhrkamp

Chapter 1

Summary

Synaptic short- and long-term plasticity are key mechanisms by which neuronal ensembles store information. The mossy fiber synapse (MF-CA3 synapse) is formed by axons of dentate gyrus granule cells and exhibits a striking form of short-term plasticity that is distinct from most other synapses in the CNS. Stimulation of mossy fiber axons at low frequencies (0.1 - 10 Hz) causes a dramatic increase in glutamate release at the MF-CA3 synapse, and a concomitant augmentation of the excitatory postsynaptic potentials. This phenomenon is called *frequency facilitation*. The mechanisms of frequency facilitation are currently under discussion.

We therefore tested the role of Ca^{2+} in the mediation of frequency facilitation at MF-CA3 synapses and found frequency facilitation independent of an accumulation of bulk Ca^{2+}. We tested the effect of blocking N- and P/Q-type voltage gated Ca^{2+} channels on frequency facilitation and found both channels contributing equally to the expression of frequency facilitiaton.
Because of the complex behavior of frequency facilitation from the extracellular Ca^{2+} concentration, we tested different mathematical models to explain this form of plasticity. A model with two distinct Ca^{2+} sensors, one responsible for basal transmitter release while the other one causes facilitation of release, described best our data.

We furthermore tested the role of different signalling pathways that are known to affect transmitter release and other forms short-term plasticity. Facilitation was unaltered in mice lacking functional αCamKII, or following application of CamKII blockers. It was also unaffected by inhibition of protein kinase A (PKA), protein kinase C (PKC), mitogen-activated protein kinase (MAPK), phosphatases, Kainate receptors (KARs), phosphatidyl-inositol kinase 3 and 4 (PI-3 and PI-4 kinase), and agents affecting the integrity of the cytoskeleton.

These data suggest that frequency facilitation is either mediated by signalling cascades that are distinct from the ones tested in this study, or alternatively, they are consistent with a more direct Ca^{2+}-dependent mechanism acting directly on the release machinery.

Chapter 2

Introduction

In 1957 Scoville and Milner presented the case of the patient H.M. who suffered from severe epilepsy. In order to remove the focus of his seizures the hippocampus and other parts of the temporal lobe were surgically removed bilaterally. A totally unexpected consequence was the loss of the ability to form new memories, a phenomenon called *anterograde amnesia*.

A crucial role of the hippocampus in memory formation was concluded from this and has been corroborated later in numerous studies (for review: Squire and Zola-Morgan, 1991). Furthermore, the rodent hippocampus has become the most important model system for investigators to understand the neuronal basis of learning and memory in the past decades.

2.1 Anatomical structure of the rodent hippocampus

The hippocampus is a part of the telencephalon and belongs functionally to the limbic system. It is most commonly subdivided into six regions, based on their cytoarchitecture: dentate gyrus (DG), hippocampus proper, subiculum, parasubiculum,

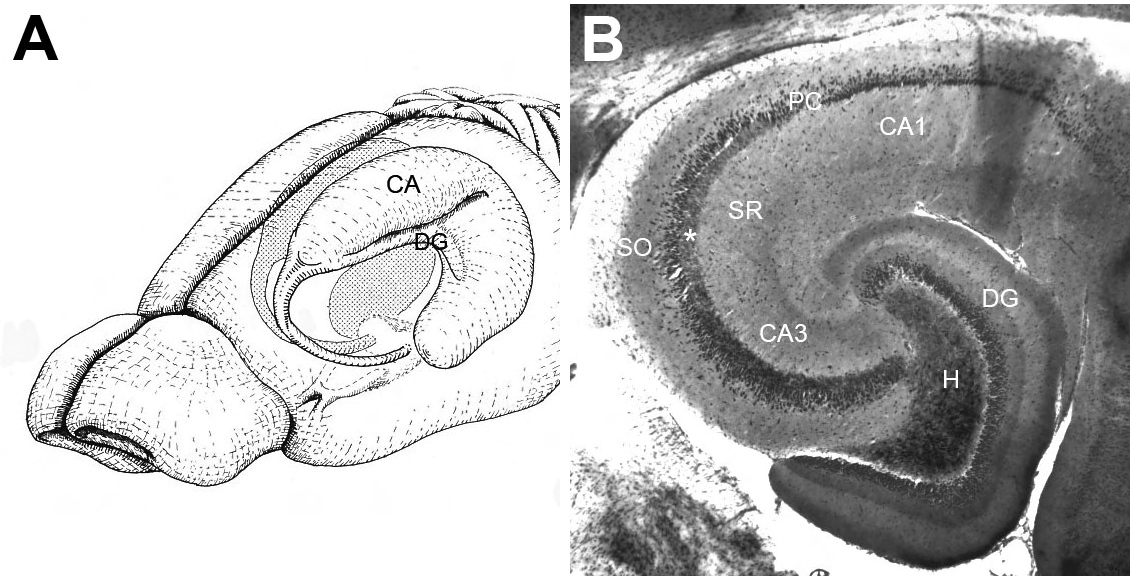

Figure 2.1: ***Anatomical view of the hippocampus.*** **A** Illustrates the position of the hippocampus in the rodent forebrain. Depicted are *cornu amonis* (CA) and dentate gyrus (DG). Part of the isocortex is removed to show the location of the hippocampus[2]. **B** Combined hematoxylin-eosin and Timm-staining of a horizontal slice from a mouse hippocampus. Dentate gyrus (DG), hilus (H), *stratum oriens* (SO), *stratum radiatum* (SR), and *stratum lucidum* (asterisk) are indicated. Note the intense staining of mossy fibers in *stratum lucidum* and *hilus* (dark grey staining).

presubiculum, and entorhinal cortex. The hippocampus proper, also called *cornu amonis* (CA), can be further divided into the areas CA1, CA2, and CA3 (Fig.2.1A). In evolutionary terms, the hippocampus belongs to the archaecortex. It has a three laminar organisation, which stands in contrast to the neocortex that exhibits a six laminar organisation.

Because of the relative simple laminar organisation (Fig.2.1B), the hippocampus proper and the adjacent dentate gyrus are ideal model systems for electrophysiological recordings. The somata of the principal neurons form a single cell layer which is surrounded by two layers containing interneurons, dendrites, and axons. The cell layer in the hippocampus proper is named *pyramidal cell layer*, because the somata

[2]adopted from: The Rat Nervous System, 2^{nd} Edition, 1994 by George T. Paxinos, Academic Press

of the principal neurons have a pyramidal like shape. Principal neurons in the dentate gyrus are named granule cells, because of their granule shaped soma.

2.2 Pathways of the hippocampus

Classically, one can distinguish three major glutamateric pathways of the hippocampus. These major pathways are (1) perforant path, (2) mossy fibers, and (3) Schaffer collaterals.
The perforant path is formed by axons of neurons in the layer II and layer III of the entorhinal cortex. These axons project to the dentate gyrus granule cells and to the pyramidal cells in area CA1 and CA3. In rodents, the perforant path connection to the dentate gyrus can be further divided functionally and pharmacologically into a lateral and a medial perforant path.

The axons of the dentate gyrus granule cells give rise to the mossy fiber pathway. The axons of the suprapyramidal blade of the mossy fiber pathway travel in a laminar manner on the same septotemporal level through the *stratum lucidum* (Claiborne et al., 1986), which is located next to the pyramidal cell layer in area CA3. Beside the projections of the mossy fiber pathway, the *stratum lucidum* also contains the proximal parts of the dendrites of the CA3 pyramidal cells. The suprapyramidal blade of the mossy fiber pathway makes synaptic connections on these apical dendrites of the pyramidal cells in CA3 and onto mossy cells in the dentate gyrus.
In contrast, the infrapyramidal blade of the mossy fiber pathway travels through *stratum oriens* (Blackstad et al., 1970) in CA3. The *stratum oriens* lies on the outer side of the pyramidal cell layer in the areas of CA3 to CA1. The *stratum oriens* contains the cell bodies of interneurons, axons, and basal dendrites of the principal cells. Synaptic contacts formed by the infrapyramidal blade of the mossy fiber pathway terminate on these basal dendrites of the pyramidal cells in area CA3.

Mossy fibers extend through the complete field of CA3 and make synaptic contacts on multiple pyramidal cells. Amaral et al. (1990) estimated that a single granule cell forms synaptic contacts onto about 14 CA3 pyramidal cells. Moreover, a single pyramidal cell is innervated by up to 50 granule cells. Because of their mossy-like appearance under a light-microscope they have been termed mossy fibers by Ramon y Cajal[3].

Unlike axons of other cortical neurons, mossy fibers form different types of synaptic contacts (Acsády et al., 1998). One type of synaptic contact is formed by large mossy fiber boutons which contact mossy cells in the hilus and the proximal parts of CA3 pyramidal cell dendrites. These synapses on CA3 pyramidal cells are termed *MF-CA3 synapses*.

The other type is a smaller synaptic contact formed along the axons of dentate gyrus granule cells. These synaptic contacts innervate interneurons in CA3 and the hilus. They can either be arranged *en passant* or are located at the end of filopodial extensions that arise from the mossy fiber boutons.

Mossy fiber boutons are large extensions of the granule cell axons (4-10 μm diameter) and are arranged in an *en passant* manner (T. W. Blackstad and Kjaerheim, 1961). Each bouton surrounds a so called *thorny excrescence*, a postsynaptic spine on the dendrite of a CA3 pyramidal cell (Fig.2.2).

But CA3 pyramidal cells are not only innervated by the mossy fiber pathway. Another strong synaptic input is given by connections from CA3 pyramidal cells of the ipsilateral (associational pathway) and the contralateral hemisphere (commissural pathway). These two types of connections are often referred to as associational/commissural (A/C) pathway. Synapses of the A/C pathway terminate on the distal parts of CA3 pyramidal cell dendrites (Gottlieb and Cowan, 1973) and on interneurons (Deller et al., 1994).

---

[3]Histologie du systéme nerveux de l´homme et des vertébrés. Vol. 2, 1911 by Ramon y Cajal, Maloine Paris

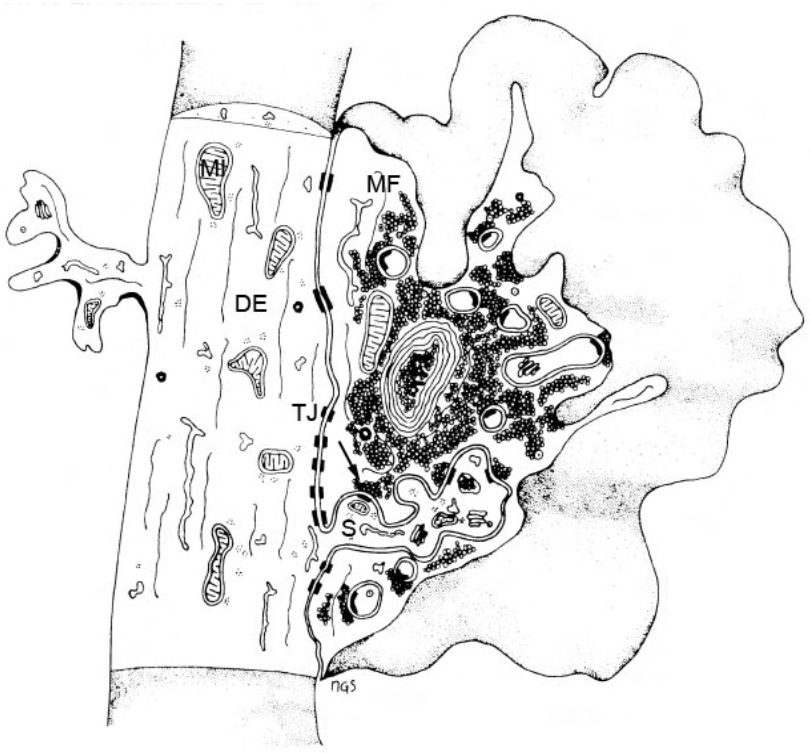

Figure 2.2: ***Schematic drawing of a mossy fiber synaptic complex.*** The mossy fiber bouton (MF) is connected to the dendritic shaft (DE) through several tight junctions (TJ). Junctions to the thorny excrescence (S) are associated with vesicles and point to release sites (arrow)[5].

Axons of the CA3 pyramidal cells project as the Schaffer collateral pathway into *stratum radiatum* and *stratum oriens* of CA1, where they synapse on apical and basal dendrites of the CA1 pyramidal cells, respectively. Collaterals also travel to the contralateral side of the brain and innervate pyramidal cells in CA1 there (Li et al., 1994). Also interneurons in CA1 are major targets of axons of the CA3 pyramidal cells (Sik et al., 1993).

Synapses formed by the Schaffer collateral pathway build the majority of intrahippocampal connections. In their review, Amaral and Witter (1989) assessed their number to be 30.000 - 60.000 synapses made by a single CA3 pyramidal cell.

[5]adopted from Amaral and Dent (1981)

2.3 Synapses

First described by Ramón y Cajal[6] it was Charles Sherrington[7] who termed the specialized connection between neurons, across which the cells communicate with each other, *synapse*. It took about four decades to introduce the idea that not all synapses function through direct electric signalling (electric synapses). Otto Loewi (1921) could show, that at the frog vagus nerve a chemical transmitter is involved in the signalling between cells. Today it is known, that these transmitter molecules are released from the presynapse, diffuse through the extracellular space, and bind to specialized receptors at the postsynapse.

2.3.1 Synaptic Function

A chemical synapse, like the MF-CA3 synapse, consists of a presynapse and postsynapse. An action potential in the presynaptic neuron travels along the efferent axon and enters the presynaptic terminal. The potential change at the presynaptic membrane leads to the opening of voltage gated Ca^{2+} channels. The following influx of Ca^{2+} ions initiates the fusion of the synaptic vesicles with the presynaptic membrane. These synaptic vesicles have a diameter of about 20 nm and contain messenger molecules, so called *neurotransmitters*. After vesicle fusion, the neurotransmitter is released to the synaptic cleft. The synaptic cleft has a distance of about 100 nm and separates the presynapse from the postsynapse.
After diffusion through the cleft, the neurotransmitter binds to specific receptors at the postsynaptic membrane. There are two types of receptors: Ionotropic receptors are ligand-gated ion channels which open upon binding the transmitter.

[6]Histologie du systéme nerveux de l´homme et des vertébrés, Vol. 2, 1911 by Ramon y Cajal, Maloine Paris

[7]A Textbook of Physiology, Vol.3: The Central Nervous System, 1897 by Michael Foster and assisted by Charles S. Sherrington

Metabotropic receptors are G-coupled receptors that act on ion channels or alter intracellular metabolic reactions.

If the neurotransmitter binds to an ionotropic receptor at the postsynaptic membrane, the resulting influx of cations leads to potential changes at the postsynaptic membrane. These potential changes can either be excitatory or inhibitory, depending on the type of synapse that is involved. Inhibitory and excitatory synapses release different kinds of neurotransmitters. The main inhibitory neurotransmitter in the hippocampus is GABA ($\gamma\ amino-butric-acid$), the main excitatory transmitter is L-glutamate.

GABA receptors come in two classes: $GABA_A$ receptors are ligand-gated chloride channels, whereas $GABA_B$ receptors are G-protein coupled receptors. The opening of $GABA_A$ receptors increases the membrane conductance for chloride and decreases the excitability of the postsynaptic neuron, because it keeps the membrane potential near its resting potential.

In contrast, glutamate receptors are cation channels and the opening causes the influx of cations into the postsynaptic terminal. This leads to a depolarisation of the postsynaptic membrane and increases its excitability.

2.3.2 Molecular mechanisms of synaptic transmission

In electron microscopy studies investigators found an electron dense structure located opposite of the synaptic cleft at the presynaptic plasma membrane. It was termed *active zone*. Several proteins have been identified that form the active zone: Munc13s, RIMs (Rab-3 interacting molecules), Piccolo, Bassoon, ERCs (ELKS/Rab-3 interacting molecules/CAST), RIM-BPs (RIM binding proteins), and α-liprins (for review: Südhof, 2004).

Docked at the plasma membrane at the active zone of a MF-CA3 synapse 8 - 10 vesicles can be found (Suyama et al., 2007). These vesicles correlate to the readily releasable pool (RRP) (Schneggenburger et al., 1999). The initial synaptic depression seen during high frequency stimulation reflects the depletion of this pool. This pool

is relative small compared to the total amount of synaptic vesicles (approximately 6 %).

Clustered at the active zone there are different types of voltage-gated Ca^{2+} channels. After arrival of an action potential these channels open. Ca^{2+} ions enter the synaptic terminal and initially occupy a relative small area around the intracellular mouth of the channel. During this period (approximately 1 ms), the Ca^{2+} concentrations around the mouth of the channel can reach concentrations of more than 10 μM. These loci of high Ca^{2+} concentrations are termed Ca^{2+} microdomains (Llinás et al., 1994) and are thought to underlie basal transmitter release.

With time, Ca^{2+} ions diffuse away from the microdomains and produce Ca^{2+} concentrations inside the terminal of about 1 μM (bulk Ca^{2+}). This is still ten-times higher than under resting conditions (Helmchen et al., 1997).

SNARE (soluble N-ethyl-sensitive-factor attachment receptor-complexes) proteins are involved in the fusion of the synaptic vesicle membrane and the membrane of the active zone. These proteins are located at both membranes. Three SNARE proteins are known to be involved in the exocytosis: Synaptobrevin at the vesicle membrane, and SNAP-25 and syntaxin-1 at the plasma membrane (Jahn et al., 2003). These proteins form unstable core complexes in which the membranes of the vesicle and the active zone have been pulled close together but have not fused. Complexin binding to these core complexes is not essential but might promote the binding of synaptotagmin (Reim et al., 2001). The formation of SNARE complexes is controlled by a group of SM-proteins (SEC1/Munc18-like proteins), among them Munc18-1 (Dulubova et al., 1999).

At the neuromuscular junction, there is a non-linear dependence of transmitter release from the intracellular Ca^{2+} concentration. Binding of several Ca^{2+} ions at a Ca^{2+} sensor has been proposed to be necessary for the induction of transmitter release (Dodge and Rahamimoff, 1967). A study of Schneggenburger and Neher (2000) on the correlation between Ca^{2+} influx and exocytosis revealed a low affinity Ca^{2+} sensor with four to five binding sites to be responsible for exocytosis at the

calyx of held.

In the past several years, it has become most probably that synaptotagmin-1 and -2 are the main Ca^{2+} sensor molecules responsible for transmitter release (for review: Bennett, 1999; Meinrenken et al., 2003). Synaptotagmins possess two Ca^{2+} binding domains. The C2A-domain binds up to three Ca^{2+} ions, the C2B-domain up to two. Therefore, the number of Ca^{2+} ions that can bind to synaptotagmin correlates to the Ca^{2+} sensor proposed for the Calyx of Held.

It seems feasible to assume that synaptotagmin binds to SNARE complexes even in the absence of Ca^{2+}. If synaptotagmin binds Ca^{2+}, the fusion of vesicle and presynaptic membrane is induced.

After fusion, the neurotransmitter is released in the synaptic cleft and the vesicle can be recycled for re-use. Three different mechanisms of vesicle recycling have been proposed. Following exocytosis, a subpopulation of vesicles are refilled locally with new neurotransmitters and stay in the RRP (*kiss-and-stay*)(Barker et al., 1972). Alternatively, it has been shown by Ceccarelli et al. (1973), that vesicles can quickly be recycled by a clathrin independent mechanism (*kiss-and-run*). Finally, vesicles can be recycled via clathrin-coated pits by fusion with the endosomal compartment (Heuser and Reese, 1973). In the later cases, vesicles are removed from the presynaptic membrane and thereby from the RRP. Moreover, these vesicles enter a different vesicle pool located at some distance ($\approx$ 250 nm) from the membrane. This reserve pool includes nearly half of all vesicles of an active zone at a MF-CA3 synapse (Suyama et al., 2007). Vesicles of this pool have do dock to the presynaptic membrane and to run through a process called *priming* before they become available for transmitter release.

To maintain the organization of the vesicles and to guide their trafficking inside the synaptic terminal vesicles are tethered to actin filaments (f-actin) through synapsin. Synapsins are a family of phosphoproteins with three isoforms expressed in vertebrates (for review: Hilfiker et al., 1999). Synapsins interact with lipid and protein components at the vesicle membrane, as well as with f-actin in the presynapse

(Rosahl et al., 1993, 1995; Ryan et al., 1996).

2.3.3 Regulation of synaptic transmission by presynaptic enzymes

Different presynaptic enzymes are known to interact with the release of neurotransmitters and have been shown to influence synaptic plasticity.
In contrast to other synapses of the hippocampus, LTP (long term potentiation) at the MF-CA3 synapse is induced and expressed presynaptically. Weisskopf et al. (1994) showed that LTP at this synapse is induced by a Ca^{2+} dependent activation of the adenylate cyclase. Adenylate cyclase catalyses the formation of cAMP from 5'-ATP. 5'-ATP in turn activates the protein kinase A (PKA), which causes a persistent increase in synaptic strength.
Moreover, it has been shown that the LTP deficient phenotype observed in a mouse model for Neurofibromatosis Type 1 is due to an excessive Ras activity. Ras is known to activate the mitogen-activated-protein kinase (MAPK). Interestingly, a common substrate for PKA and MAPK are synapsins.

Also forms of short-term synaptic plasticity (STP) have been shown to be regulated by enzymatic functions. Frequency facilitation at the MF-CA3 synapse has been shown to be reduced by application of blockers for CamKII. Two CamKII isoforms are expressed in the hippocampus: αCamKII and βCamKII. αCamKII is a protein kinase that is ubiquitously expressed in neurons. It is highly enriched in the hippocampus and neocortex and is present at the presynaptic and the postsynaptic side. At the postsynaptic side, αCamKII is part of the postsynaptic density (PSD), an electron dense structure at synaptic release sites. αCamKII phosphorylates beside others also synapsins in a Ca^{2+} dependent manner.
αCamKII has been found to be involved critically in several forms of synaptic plasticity, among them frequency facilitation at MF-CA3 synapses (Salin et al., 1996). Moreover, experiments with αCamKII deficient mice revealed a loss of NMDAR-

dependent LTP in the CA1 region (Elgersma et al., 2002; Silva et al., 1992) and altered metaplasticity in the dentate gyrus (Zhang et al., 2005). Furthermore, Stanton and Gage (1996) could show by local application of CamKII inhibitors that presynaptically located αCamKII is involved in the expression of long-term depression (LTD) at the CA3-CA1 synapse. In addition, a non-enzymatic function of presynaptic αCamKII at the CA3-CA1 synapse was suggested by Hojjati et al. (2007). These authors could show that the regulation of the number of docked vesicles by αCamKII is independent of its enzymatic function.

Another interesting enzyme that has been found to be involved in synaptic plasticity is NCS-1 (Neuronal Ca^{2+} Sensor-1). Sippy et al. (2003) showed in hippocampal cell cultures, that overexpression of NCS-1 can switch paired-pulse depression to facilitation. NCS-1 is the mammalian homologue of the *drosophila* frequenin (Pongs et al., 1993). In endocrine cells NCS-1 interacts with the phosphatidyl-inositol-4-kinase. This kinase is involved in phosphatidyl-inositol signalling (see Fig.2.3 for details). Inositol-1,4,5-triphosphate (IP_3) is an important second messenger in nerve cells (Iino, 2006). It is hydrolysed of phospholipids of the inner leaflet of the plasma membrane by phospholipase C (PLC). In this reaction diacylglycerol (DAG) and IP_3 are formed. Whereas DAG activates protein kinase C (PKC), IP_3 is known to release Ca^{2+} from intracellular stores.

Synapses with a low release probability preferentially express high levels of short-term facilitation, whereas synapses with a high release probability preferentially show short-term depression (Dobrunz and Stevens, 1997). Therefore, it has been suggested that MF-CA3 synapses possess an initially rather low release probability. This low release probability is maintained by tonic activation the G-protein coupled A_1 receptor (adenosine receptor) (Moore et al., 2003). Interestingly, it has also been reported that there is no influence of A_1 receptor on synaptic plasticity at the MF-CA3 synapse (Kukley et al., 2005). In their study, Kukley et al. (2005) suggest, that hypoxia is causing this obvious controversy. The authors argue, that under metabolic stress, like hypoxia, adenosine is released in the extracellular space and

activates A_1 receptors. Because Moore et al. (2003) used an submerged chamber for their experiments, it is feasible to assume that this could cause an insufficient oxygen supply of the brain slice and a subsequent unphysiological high extracellular adenosine concentration. In contrast, Kukley et al. (2005) performed their experiments with an interface chamber. It has been shown, that the oxygen supply in interface chambers is better compared to submerged chambers. These findings make it most likely, that A_1 receptors are not involved in the induction of MF-CA3 frequency facilitation.

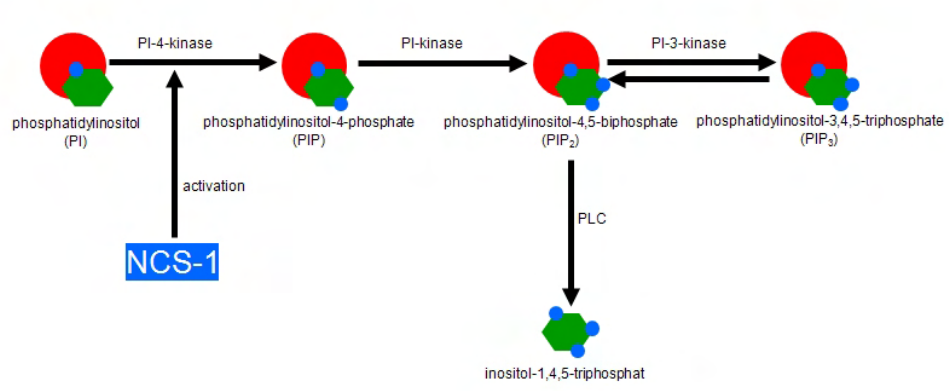

Figure 2.3: ***Simplified depiction of the phosphatidyl-inositol (PI) pathway.*** NCS-1 activates PI-4-kinase that converts PI into phosphatidyl-4-phosphate (PIP). PIP can be transformed into PIP_2 by PI-kinase. PIP_2 can either be cleaved into inositol-1,4,5-triphosphate by phospholipase C (PLC) or into PIP_3 by PI-3 kinase.

2.3.4 Glutamate receptors at the MF-CA3 synapse

The MF-CA3 synapse is an excitatory synapse. Three major subtypes of ionotropic glutamate receptors are expressed at this synapse: AMPA (α-amino-3-hydroxy-5-methylisoxazol-4-proprionic acid), KA (kainate-acid), and NMDA (*N*-methyl-D-aspartate) receptors (AMPAR, KAR, and NMDAR). These receptors are named for the specific synthetic agents that activate them.

AMPA and KA receptors are abundantly expressed at the MF-CA3 synapse, whereas

NMDA receptors are less expressed than at other cortical synapses (Lei and McBain, 2002). Moreover, it has been postulated that NMDARs might be located extrasynaptically and are activated by glutamate spill-over.
Whereas AMPARs and NMDARs are mainly expressed at the postsynaptic side, it was shown that the KAR subtypes Glu_{K1} and Glu_{K2} are expressed at mossy fiber boutons (Darstein et al., 2003). Several studies suggested a role of presynaptic KA autoreceptors in MF-CA3 frequency facilitation (Breustedt and Schmitz, 2004; Contractor et al., 2001; Kamiya et al., 2002; Lauri et al., 2003; Schmitz et al., 2001), but also see (Kwon and Castillo, 2008).
In addition, there are metabotropic glutamate receptors (mGluRs) expressed at both, pre- and postsynaptic side of MF-CA3 synapses, namely mGluR1b/5 (group I), mGluR2/3 (group II), and mGluR4a (group III) (Abe et al., 1992).

2.3.5 Short-term synaptic plasticity

While electrical synapses show a rather limited capability of modifying transmission, chemical synaptic transmission is highly regulated. Most chemical synapses in the CNS have the ability to adapt their transmission efficacy depending on the presynaptic activation pattern (for review: Bear and Malenka, 1994; Cavazzini et al., 2005; Nicoll and Schmitz, 2005; Shain and Carpenter, 1981).
This process of modulation is called *synaptic plasticity*. A modification of transmission is possible in both directions. This can lead to synaptic depression or potentiation, respectively.

One form of short-term synaptic plasticity is facilitation. Facilitation is thought to be induced and expressed mainly at the presynaptic side, a potential involvement of postsynaptic processes seems to be rather negligible (for review: Fisher et al., 1997; Zucker and Regehr, 2002).
Since the initial experiments of Katz and Miledi (1968) showing a crucial role of extracellular Ca^{2+} for synaptic transmission and facilitation at the neuromuscular

junction, a Ca^{2+} based mechanism has been favored for the induction of facilitation. Generally, it has been thought that Ca^{2+} ions entering the presynaptic terminal cause the release of neurotransmitters, but can also lead to an increase of the amount of released neurotransmitters during repetitive stimulations. This increase could be achieved by having more available quanta (vesicles) for release or by an increased probability, with which a vesicle will fuse upon stimulation. Whereas the number of available quanta can be controlled e.g. by regulating the size of the RRP, a reason for an increased release probability could be an augmented influx of Ca^{2+} ions, increased affinity of the Ca^{2+} sensor, or a closer coupling of this sensor to the Ca^{2+} influx site (for review: Zucker and Regehr, 2002).
The *residual Ca^{2+} hypothesis* (Katz and Miledi, 1968) explained the phenomenon of facilitation at the neuromuscular junctions by an accumulation of bulk Ca^{2+} ions in the presynaptic terminal. If Ca^{2+} ions from a prior stimulation are not completely removed from the presynaptic terminal before the arrival of the next action potential, the Ca^{2+} ions accumulate and increase the probability of release.
However, measurements of presynaptic bulk Ca^{2+} concentrations revealed that this hypothesis is not suitable to explain certain other forms of synaptic plasticity. Tetanic stimulation pattern induce a form of synaptic plasticity that is called *post-tetanic potentiation* (PTP). This potentiation can last for several minutes (Delaney et al., 1989). Because bulk Ca^{2+} concentrations reach resting levels already after several seconds (Shimizu et al., 2008), an accumulation of bulk Ca^{2+} cannot explain this form of plasticity.

MF-CA3 synapses are rather unique in the expression of various forms of STP (for review: Nicoll and Schmitz, 2005). One very prominent form of STP at the MF-CA3 synapse is frequency facilitation. Frequency facilitation is induced by repetitive stimulations of the axons of dentate gyrus granule cells. This stimulation leads to a profound increase in the amount of transmitter release and a subsequent increase of the EPSP (excitatory postsynaptic potential) amplitude. Interestingly, facilitation can be observed even at rather low stimulation frequencies (0.1 - 10 Hz) (Salin et al.,

1996).

Beside frequency facilitation, paired-pulse facilitation is another very prominent form of STP at the MF-CA3 synapse. Temporal pairing of two stimuli results in a strong potentiation of the EPSP amplitude at the second stimulation (Salin et al., 1996). The amount of frequency and paired-pulse facilitation at the MF-CA3 synapse is much higher than at other cortical synapses.

These forms of STP might be relevant to integrate presynaptic activity (for review: Urban et al., 2001). Indeed, dentate gyrus granule cells are known to show low frequency firing which could induce frequency facilitation under physiological conditions (Gundlfinger et al., 2007; Leibold et al., 2008; Moser et al., 1993)(for review: Nicoll and Schmitz, 2005).

The mechanisms underlying frequency facilitation and paired-pulse facilitation are still under discussion.

2.4 Aim of the work

So far it remained clear, that frequency facilitation at MF-CA3 synapses seems to be induced and expressed presynaptically as an increase in the amount of released neurotransmitters. Further details about the underlying mechanisms are ambiguous.

In the last years several mechanisms have been suggested to participate in frequency facilitation at the MF-CA3 synapse, among them activation of αCamKII (Salin et al., 1996), activation of presynaptic KA autoreceptors (Breustedt and Schmitz, 2004; Contractor et al., 2001; Kamiya et al., 2002; Lauri et al., 2003; Schmitz et al., 2001), and high endogenous Ca^{2+} buffer concentration (Blatow et al., 2003). Non of them has been unequivocally proven.

This work intended to identify and characterize the mechanisms leading to frequency facilitation at the MF-CA3 synapse. To investigate frequency facilitation we measured extracellular field-EPSPs (fEPSPs) recorded in *stratum lucidum* of the murine hippocampus.

Chapter 3

Materials and Methods

3.1 Preparation of animals

Male Bl6/N mice (28 - 40 days old) were obtained from Charles River (Sulzfeld, Germany). In some experiments we used αCamKII knock-out mice (αCamKIIdeltaEX2), provided by Ype Elgersma, Erasmus MC Rotterdam, The Netherlands. These animals were αCamKII null mice in which the exon 2 of the αCamKII gene had been deleted. As a result, these animals have been shown to express no CamKII activity with an unchanged expression level of βCamKII (Elgersma et al., 2002).

For preparation, animals were anesthetized using a mixture of Ketamine (Upjohn, Heppenheim, Germany: 100 mg/kg, i.p.) and Xylazin (Bayer, Leverkusen, Germany: 80 mg/kg, i.p.). Animals have been heart-perfused with ice-cold carbogenated (95 % O_2 / 5 % CO_2) dissection saline containing the following (in mM): 40 NaCl, 150 sucrose, 25 $NaHCO_3$, 1.25 NaH_2PO_4, 3 KCl, 0.5 $CaCl_2$, 7 $MgCl_2$, 25 glucose, pH 7.4. The brain was quickly removed and immediately submerged in ice-cold dissection saline. Four hundred micrometer thick horizontal slices were prepared using a vibratome (either a VT 1000S, Leica, Wetzlar, Germany or a Microm HM650V, Walldorf, Germany). The slices have been transferred into a holding

chamber or directly into an interface chamber for recordings. They have been continuously superfused with ACSF (2 ml/min) consisting of (in mM): 125 NaCl, 26 $NaHCO_3$, 1.25 NaH_2PO_4, 3 KCl, 2.5 $CaCl_2$, 1.3 $MgCl_2$, 25 glucose, pH 7.4, gassed with 95% O_2 and 5% CO_2. Slices were allowed to recover for at least 1 hour before starting the experiment. The temperature in the interface chamber was kept constant at 35°C ± 1°C.

3.2 Electrophysiology

Extracellular recording and stimulation electrodes were manufactured from borosilicate glass (GB150-8P, Science Products, Hofheim, Germany) on a vertical puller (PP-830, Narishige, Tokyo, Japan). The electrodes had a resistance of approximately 2 MΩ when filled with ACSF.

For recording of mossy fiber fEPSPs (MF-fEPSPs), stimulation and recording electrodes were placed at approximately 150 μM distance between both electrodes in the *stratum lucidum*.

The stimulation induces an action potential in the axons of dentate gyrus granule cells. The action potential causes the opening of voltage gated Ca^{2+} channels at mossy fiber boutons and a subsequent release of neurotransmitters (L-glutamate). The neurotransmitters bind to ionotropic glutamate receptors at the postsynaptic membrane and cause the influx of cations into CA3 pyramidal cells. This local current flow induces potential changes between our recording electrode near the pyramidal cell layer and our reference electrode in the bath (ground).

Because of the small resistivity of the extracellular space, potential changes caused by single synapses are too small to be detected. Therefore, we needed simultaneous activation of many MF-CA3 synapses to produce detectable potential changes between recording and reference electrode. Because the principal cells in the hippocampus are arranged in a laminar organisation, the hippocampus provides an ideal setting to provide summation of synaptic potentials.

Stimulation was performed with square pulses (5 - 20 μA) of 100 μs duration (A360 Stimulus Isolator, World Precision Instruments, Sarasota, USA). To assess frequency facilitation, trains of 15 double pulse stimulations (40 ms interstimulus interval, ISI) at 1 Hz or 0.3 Hz were delivered. Signals were amplified 100 times (BF48DGX, NPI, Tamm, Germany), filtered (3 kHz lowpass) with an Axoclamp 2B amplifier (additional ten times amplification)(Molecular Devices, Foster City, USA), and digitized at 10 kHz sampling rate (Digidata 1200A, Molecular Devices, Foster City, USA). Data were aquired using pClamp7.0 software (Molecular Devices, Foster City, USA) and analyzed with Clampfit9.2 software (Molecular Devices, Foster City, USA), Excel 2003 (Microsoft, Redmond, USA), and Igor Pro 6.03 (Wavemetrics, Nimbus, USA).

In some experiments, the Ca^{2+} concentration in the ACSF was altered. In these Experiments, we adjusted the extracellular Mg^{2+} concentration to keep the divalent cation concentration in the ACSF constant as follows (in mM): 0.9 Ca^{2+}/2.9 Mg^{2+} , 1.5 Ca^{2+}/2.3 Mg^{2+}, 2.5 Ca^{2+}/1.3 Mg^{2+}, 3.3 Ca^{2+}/0.5 Mg^{2+}. If the Ca^{2+} concentration has been elevated to 5 and 10 mM we used HEPES buffered saline containing (in mM) 150 NaCl, 15 HEPES, 3 KCL, 2.5/5/10 $CaCl_2$, 0.3 $MgCl_2$, 22 glucose, (pH 7.4, bubbled with O_2). Note that the divalent cation concentration was not constant in the bath using this solution.

3.3 Technical problems of MF-CA3 field recordings

Brown and Johnston (1983) initially suggested the mossy fiber synapse as a model system for investigating basic synaptic physiology. Bulk stimulation of mossy fibers is relatively simple, because the axons of dentate gyrus granule cells are bundled within the *stratum lucidum* and can therefore easily be recognized.

Moreover, the MF-CA3 synapse is rather interesting because of its unique properties of STP. Unfortunately, there are some technical problems for field potential

recordings performed at the mossy fiber pathway.

Although bundled within *stratum lucidum*, it is difficult to find a stimulation site that results in exclusive MF-CA3 synaptic responses without activation of other pathways. This is due to the sparse connectivity of DG granule cells to CA3 pyramidal cells (Claiborne et al., 1986).
In addition, extracellular stimulation of axons in *stratum lucidum* can result in additional activation of other synaptic inputs onto CA3 pyramidal cells, even if an exclusive stimulation of mossy fibers is achieved. CA3 pyramidal cells form recurrent connections among each other, thus a suprathreshold excitation of a pyramidal cell can lead to EPSPs in other pyramidal cells via recurrent axons. Therefore, it is not uncommon to detect bisynaptically induced EPSPs in a electrophysiological measurement.
Beside that, an anti/orthodromic mechanism can be present. Stimulation of mossy fiber axons can induce an antidromic activation of granule cell axon collaterals in the hilus. This can lead to a secondary orthodromic activation of MF-CA3 inputs on pyramidal cells in CA3. Although this is an exclusive MF-CA3 activation, the synaptic potentials will have complex kinetics. This makes the analysis difficult. Stimulation of axon collaterals can also induce activation of hilar interneurons that give rise to non-mossy fiber synaptic input onto pyramidal cells in CA3.

Because of these possible contaminations in the recorded signal, diverse criteria have been established to identify pure, monosynaptic MF-CA3 synaptic inputs.
We established two criteria that had to be fulfilled before the start of each experiment. Firstly, paired-pulse facilitation (determined as the ratio between the second and the first fEPSP amplitude elicited by a paired stimulation with an ISI of 40 ms) had to be 250 %. Secondly, stimulation of mossy fibers at 1 Hz had to cause facilitation of the MF-fEPSPs of at least 450 %.
Finally, after each experiment the selective group II mGluR agonist DCG-IV ((2S,2'R,3'R)-2-(2',3'-dicarboxycyclopropyl)glycine) (3 μM) was applied. The group II metabotropic glutamate receptor 2 (mGluR2) is exclusively expressed on large mossy fiber boutons

but not on synapses of the A/C pathway (Kamiya et al., 1996). The A/C pathway is known to cause most contaminations of MF-fEPSP recordings. Application of DCG-IV leads to inhibition of presynaptic voltage-gated Ca^{2+} channels and thereby to a substantial decrease of transmitter release from MF-CA3 synapses. This causes a potent rerduction of the MF-fEPSP amplitudes. If the application of DCG-IV caused a reduction of MF-fEPSP amplitudes of > 80 %, the experiment was used for further analysis.

For recordings of Schaffer-collateral fEPSPs (SC-fEPSPs), stimulation and recording electrodes were placed in the *stratum radiatum* of CA1 at approximately 200 μm distance from each other.

3.4 Drugs and reagents

All compounds used for the preparation of solutions were obtained from Sigma-Aldrich (Deisenhofen, Germany).
All other substances were stored as stock solutions in the appropriate solvent at -25 °C (see Table 3.1). For experimental use, stocks have been diluted into ACSF to get the final concentration. 0.1 % cytochrome C (Sigma-Aldrich, Deisenhofen, Germany) has been added to the ACSF before ω-conotoxin GVIa or agatoxin IVa was diluted.

substance	**vendor**	**solvent**	**final conc.**
agatoxin IVa	Bachem, Weil am Rhein, Germany	ACSF	200 nM
ω-conotoxin GVIa	Bachem, Weil am Rhein, Germany	ACSF	2 μM
cyclosporin	Tocris, Bristol, UK	DMSO	200 μM
DCG-IV	Tocris, Bristol, UK	ACSF	3 μM
EGTA-AM	Merck, Darmstadt, Germany	DMSO	100 μM
jasplakinolide	Tocris, Bristol, UK,	DMSO	200 nM
KN-62	Tocris, Bristol, UK,	DMSO	10 μM
KN-93	Tocris, Bristol, UK,	DMSO	3.5 μM
latrunkulin A	Tocris, Bristol, UK,	DMSO	5 μM
PD98056	Tocris, Bristol, UK,	DMSO	50 μM
RP-cAMPs	Tocris, Bristol, UK,	DMSO	100 μM
Staurosporin	Tocris, Bristol, UK,	DMSO	200 nM
U73122	Tocris, Bristol, UK,	DMSO	20 μM
UO126	Tocris, Bristol, UK,	DMSO	20 μM
Wortmannin	Tocris, Bristol, UK,	DMSO	200 nM or 1 μM
NS-102	Tocris, Bristol, UK,	ACSF	10 μM

Figure 3.1: ***Pharmacological agents.*** The table indicates the origin of the drugs purchased for this study. In addition, the appropriate solvents and final concentrations for use in the experiments are noted.

Chapter 4

Results

4.1 Short-term plasticity at the MF-CA3 synapse

MF-CA3 synapses express a unique form of potentiation at low stimulation frequencies called *frequency facilitation* (Salin et al., 1996) (for review: Nicoll and Schmitz, 2005). Because the mechanisms underlying frequency facilitation are still under debate, we investigated frequency facilitation at MF-CA3 synapses of the murine hippocampus.

MF-fEPSPs exhibited pronounced paired-pulse facilitation to the second of two closely (10 - 500 ms) timed stimuli (250.9 % ± 10.6 %, n = 5, at 40 ms ISI, Fig.4.1A). Interestingly, there was still pronounced facilitation detectable at ISIs > 300 ms. Thus, these synapses show pronounced facilitation when mossy fibers are stimulated at low stimulation frequencies.

During stimulation at 0.3 Hz, there was a strong potentiation of the MF-fEPSP amplitudes present which rapidly increased during a stimulation train with an exponential time course. After a few stimulations amplitudes saturated (263.2 % ± 19.7 % after 15 stimulations, n = 5, Fig.4.1B and C). The potentiation was completely reversible within 30 s. With higher frequencies a stronger facilitation was seen (643.1% ± 47.3 % after 15 stimulations at 1 Hz, n = 5, Fig.4.1B and C).

These results are in agreement with published data (Blatow et al., 2003; Salin et al., 1996) (for review: Nicoll and Schmitz, 2005). We concluded, that MF-CA3 synapses indeed show two rather interesting forms of STP, namely paired-pulse facilitation and frequency facilitation.

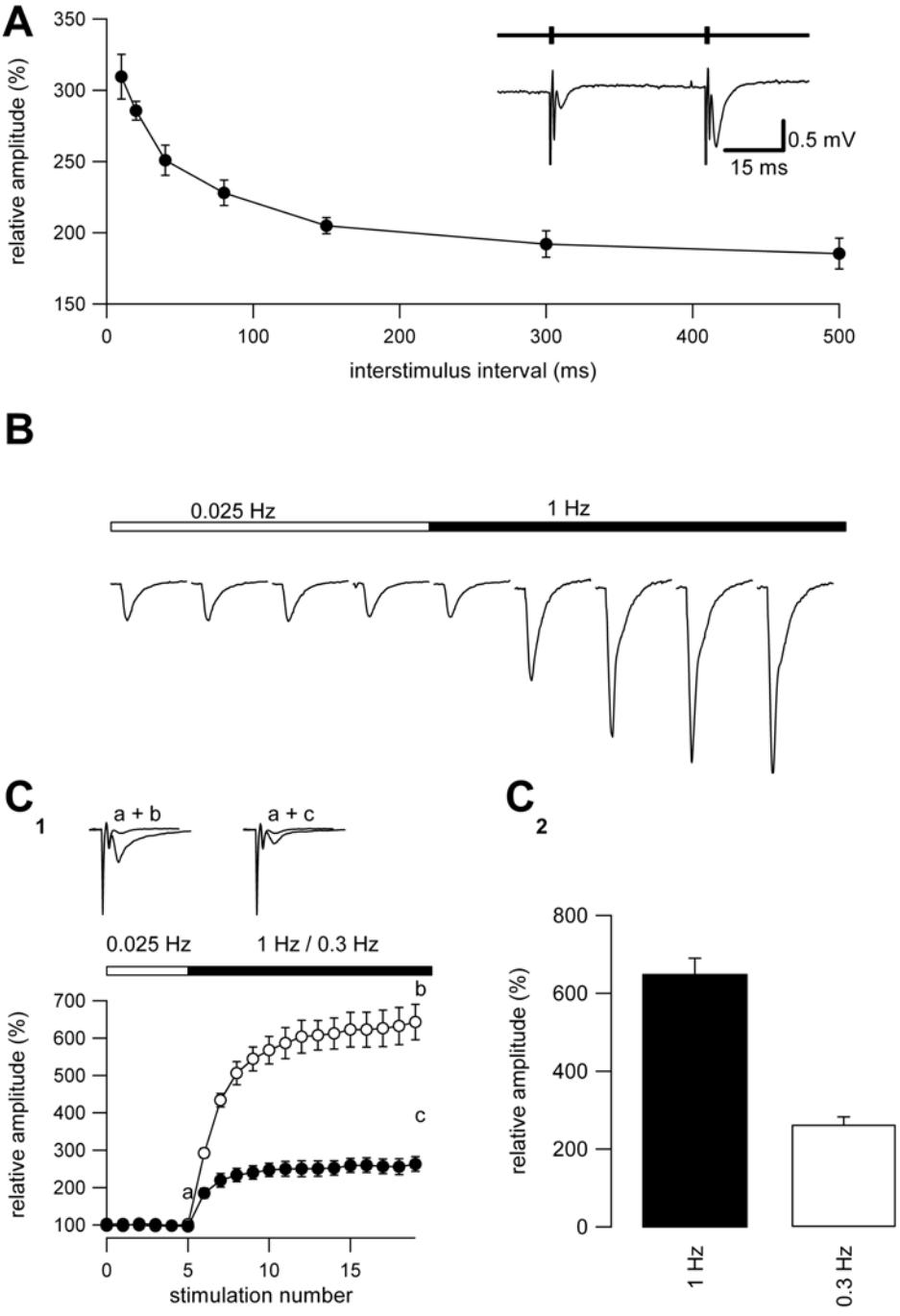

Figure 4.1: ***Short-term plasticity at the MF-CA3 synapse.*** **A** MF-CA3 synapses exhibit large levels of paired-pulse facilitation over a wide range (10 - 500 ms) of ISIs. **Inset** shows representative sample traces at 40 ms ISI and the stimulation pattern (indicated by vertical bars). Even at long ISIs significant facilitation can still be observed. **B** illustrates representative MF-fEPSPs (truncated in B **lower**) at different stimulation frequencies (**upper**). Pronounced frequency facilitation can be observed by changing the stimulation frequencies from 0.025 Hz to 1 Hz. $\mathbf{C}_1$ Time course of MF-fEPSP amplitudes (**lower**) at different stimulation frequencies (**middle**). Changing the stimulation frequency from 0.025 Hz to 1 Hz (open circles) leads to a dramatic increase in MF-fEPSP size, whereas changing from 0.025 Hz to 0.3 Hz (filled circles) leads to smaller increases in the MF-fEPSP amplitudes. **Upper** panel shows sample traces obtained at the time points indicated by the lowercase letters. $\mathbf{C}_2$ Quantification of the levels of frequency facilitation after 15 stimulations from the experiments presented in C_1 for 1 Hz (black bar) and 0.3 Hz (white bar).

4.2 An accumulation of bulk Ca^{2+} is not underlying facilitation at MF-CA3 synapses

It has previously been reported for different types of synaptic terminals and the neuromuscular junction that the influx of Ca^{2+} ions into the presynaptic terminal is underlying the expression of various forms of STP (for review: Zucker and Regehr, 2002).

Thereby, an accumulation of presynaptic bulk Ca^{2+} has been proposed to be responsible for the induction of facilitation at the neuromuscular junction (Katz and Miledi, 1968) and the squid giant axon (Zucker and Stockbridge, 1983). But there is evidence, that facilitation at other synapses does not depend on internal bulk Ca^{2+} (Blundon et al., 1993; Rozov et al., 2001).

We therefore asked, if facilitation at the MF-CA3 synapse is mediated by an accumulation of bulk Ca^{2+} inside a mossy fiber bouton. To address this question we bath applied the membrane permeable low affinity Ca^{2+} chelator ethylenglycol-bis(β-aminoethyl)-N,N,N',N'-tetraacetoxymethyl ester (EGTA-AM, 100 μM). The ester-bound form is unable to chelate Ca^{2+} ions. If the compound diffuses through

the plasma membrane, the ester is enzymatically removed and the compound becomes active EGTA. Because of its low Ca^{2+} affinity, this buffer can interfere with the slow bulk Ca^{2+} signal, but leaves Ca^{2+} microdomains intact (Adler et al., 1991; Cummings et al., 1996).
It has previously been shown that paired-pulse facilitation at the Schaffer collateral pathway is effectively blocked by the application of low affinity Ca^{2+} buffers (Blatow et al., 2003). Therefore, we simultaneously recorded fEPSPs at the Schaffer collateral pathway to control for a successful application of EGTA-AM.

We monitored the amount of paired-pulse facilitation at Schaffer collateral synapses during the bath application of EGTA-AM (Fig.4.2A_1). Whereas we observed a robust paired-pulse facilitation before application of EGTA-AM (140.3 % ± 4.4 %, n = 4, Fig.4.2A_1, and black bar in A_2), this potentiation was completely blocked after washin of the buffer (113.2 % ± 0.8 %, n = 4, Fig.4.2A_1, and white bar in A_2). This indicates that the buffer was effective to block bulk Ca^{2+} signalling.
In contrast, paired-pulse facilitation at the simultaneously recorded MF-CA3 synapses was not affected by application of EGTA-AM (308.1 % ± 24.6 %, n = 4, black bar in Fig.4.2A_2 compared to 284.3 % ± 14.6 %, n = 4, white bar in Fig.4.2A_2).

In the same experiments we investigated frequency facilitation at MF-CA3 synapses. Before application of EGTA-AM, changing our stimulation frequency from 0.025 Hz to either 1 Hz or 0.3 Hz resulted in a strong potentiation of MF-fEPSPs. Comparing the amount of frequency facilitation before and after application of EGTA-AM did not reveal changes at either 1 Hz (647.9 % ± 102.0 %, n = 3, Fig.4.2B_1, and black bar in Fig.4.2B_2, compared to 542.7 % ± 49.3 %, Fig.4.2B_1, and white bar in Fig.4.2B_1, B_2) or 0.3 Hz (297.4 % ± 27.2 %, n = 4, Fig.4.2B_1, and black bar in Fig.4.2B_2, compared to 226.8 % ± 21.3 %, Fig.4.2B_1, and white bar in Fig.4.2B_1, B_2).

These experiments suggested, that paired-pulse and frequency facilitation at MF-CA3 synapses are not mediated by an accumulation of bulk Ca^{2+} inside mossy fiber boutons. In contrast, paired-pulse facilitation at the Schaffer-collateral pathway was completely blocked by EGTA-AM.

Because Ca^{2+} microdomains are unaffected by application of low affinity Ca^{2+} buffers like EGTA-AM, it is likely that facilitation at the MF-CA3 synapse is mediated primarily by Ca^{2+} microdomains. If so, the Ca^{2+} sensor mediating paired-pulse and frequency facilitation must be located close to the Ca^{2+} entry site.

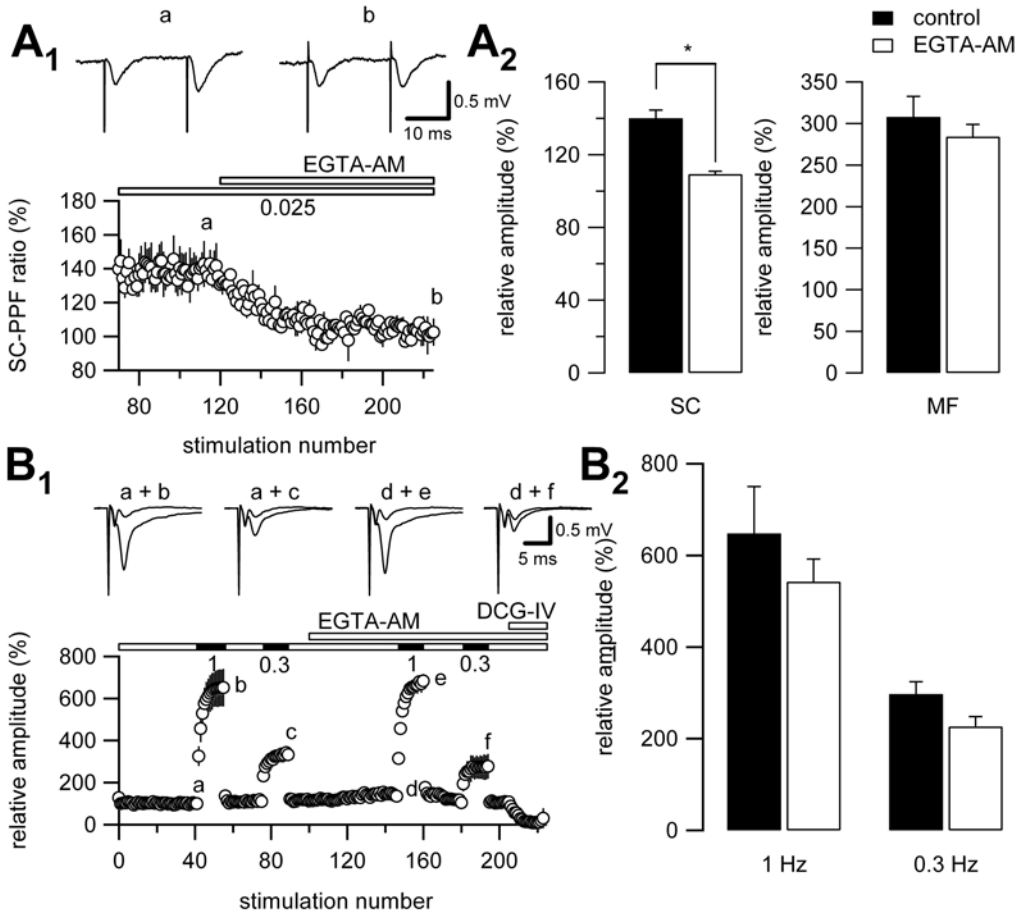

Figure 4.2: ***Frequency facilitation depends not on an accumulation of presynaptic bulk Ca^{2+}.*** $\mathbf{A}_1$ To control for a successful application of the membrane permeable Ca^{2+} chelator EGTA-AM (100 μM) we recorded paired-pulse facilitation at Schaffer-collateral (SC) synapses. **Lower** Time course of paired-pulse facilitation at SC synapses during bath application of the buffer (**middle**, white bar). Perfusing slices with EGTA-AM strongly reduced paired-pulse facilitation at these synapses. **Upper** Sample traces obtained at the time points indicated by lowercase letters. $\mathbf{A}_2$ **left** EGTA-AM (white bar) completely reduced paired-pulse facilitation at SC-synapses compared to control conditions before buffer application (black bar). Asterisk indicate significant changes in paired-pulse facilitation ($p < 0.05$). **Right** In contrast, paired-pulse facilitation recorded at MF-synapses showed no change in paired-pulse facilitation when applying EGTA-AM

(white bar) compared to control conditions (black bar). $\mathbf{B}_1$ Time course of MF-fEPSP amplitudes (**lower**) recorded in the same slices as SC-fEPSPs presented in A_1 and A_2 at different stimulation frequencies (**middle**) indicated by numerals (in Hz). Bars indicate the duration of the compound bath applications. Sample traces in the upper panel are obtained at the time points indicated by the lowercase letters. Bath application of EGTA-AM had no influence on frequency facilitation. $\mathbf{B}_2$ Summary of the amount of frequency facilitation after 15 stimulations at 1 Hz (**left**) or 0.3 Hz (**right**) from the experiments presented in B_1 for the application of EGTA-AM (white bar) and control conditions (black bar). The levels of frequency facilitation were unchanged by application of the buffer.

4.3 Ca^{2+} channel dependency of MF-CA3 frequency facilitation

4.3.1 Testing the role of N- and P/Q-type Ca^{2+} channels in frequency facilitation

We next investigated, if different Ca^{2+} channels play a role in the induction of MF-CA3 frequency facilitation. Large mossy fiber boutons express R-, P/Q-, and N-type Ca^{2+} channels (Castillo et al., 1996, 1994; Dietrich et al., 2003). It was shown by Dietrich et al. (2003), that blocking R-type channels leaves frequency facilitation at MF-CA3 synapses unaffected. Therefore, we asked if frequency facilitation at MF-CA3 synapses is influenced by blocking either P/Q- or N-type channels.

To test this hypothesis, we bath applied the selective N-type channel blocker ω-conotoxin GVIa (2 μM), the toxin of *conus geographus*. Application of the toxin reduced the amplitudes of MF-fEPSPs to 79.1 % $\pm$ 5.6 % of baseline transmission (n = 4, Fig.4.3A). Blocking N-type channels reduces the total Ca^{2+} influx at MF-CA3 synapses, because Ca^{2+} ions enter mossy fiber boutons now only through P/Q-type channels. Because the transmitter release depends on the intracellular Ca^{2+} concentration (Sakaba and Neher, 2001; Schneggenburger and Neher, 2000),

this causes a reduction of the MF-fEPSPs amplitudes. Increasing the extracellular Ca^{2+} concentration leads to an enhanced Ca^{2+} influx through the unblocked channels and thereby to an enhanced transmitter release. We increased the extracellular Ca^{2+} concentration to 3.3 or 4.1 mM Ca^{2+}, so MF-fEPSP amplitudes were comparable to baseline conditions (102.3 % ± 5.9 %, n = 4, Fig.4.3A).
The quantification of the relative amount (relative to baseline conditions) of frequency facilitation at 1 Hz showed equal amounts for all conditions (control: 728.2 % ± 33.5 %, n = 4, black bar in Fig.4.3C, ω-conotoxin: 617.0 % ± 45.7 %, n = 4, white bar Fig.4.3C, ω-conotoxin + high Ca^{2+}: 666.8 % ± 64.3 %, n = 4, hatched bar in Fig.4.3B). The same holds true for 0.3 Hz stimulation frequency, where frequency facilitation was also unchanged after blocking N-type channels (control: 276.9 % ± 12.3 %, n = 4, black bar in Fig.4.3B, ω-conotoxin: 257.5 % ± 37.5 %, n = 4, white bar Fig.4.3C, ω-conotoxin + high Ca^{2+}: 242.4 % ± 17.8 %, n = 4, hatched bar in Fig.4.3B).

We then performed an experiment, in which we applied the toxin of the funnel web spider *Agelenopsis aperta*, that selectively blocks P/Q-type Ca^{2+} channels. Application of 200 nM agatoxin IVa completely blocked synaptic transmission at MF-CA3 synapses (Fig.4.3B). Under this condition frequency facilitation was due to the dramatic reduction in Ca^{2+} influx nearly abolished. Even elevating the extracellular Ca^{2+} concentration to 8 mM only partially recovered MF-fEPSP amplitudes. The dramatic changes in baseline synaptic transmission precluded a quantitative analysis in three of these experiments, although in all experiments still a pronounced frequency facilitation could be observed. In the two experiments where a quantitative analysis was possible, frequency facilitation at 1 Hz changed from 642.6 % before application of the toxin to 1046.1 %, and from 618.6 % to 392.2 %, respectively. At 0.3 Hz we found changes in the amount of frequency facilitation from 369.3 % to 269.0 % , and from 305.7 % to 161.5 %.

As previously shown, N- and P/Q-type Ca^{2+} channels do contribute to basal synaptic transmission at MF-CA3 synapses (Castillo et al., 1996, 1994). In contrast,

we found no differential influence of blocking either P/Q- or N-type channels on frequency facilitation at theses synapses.

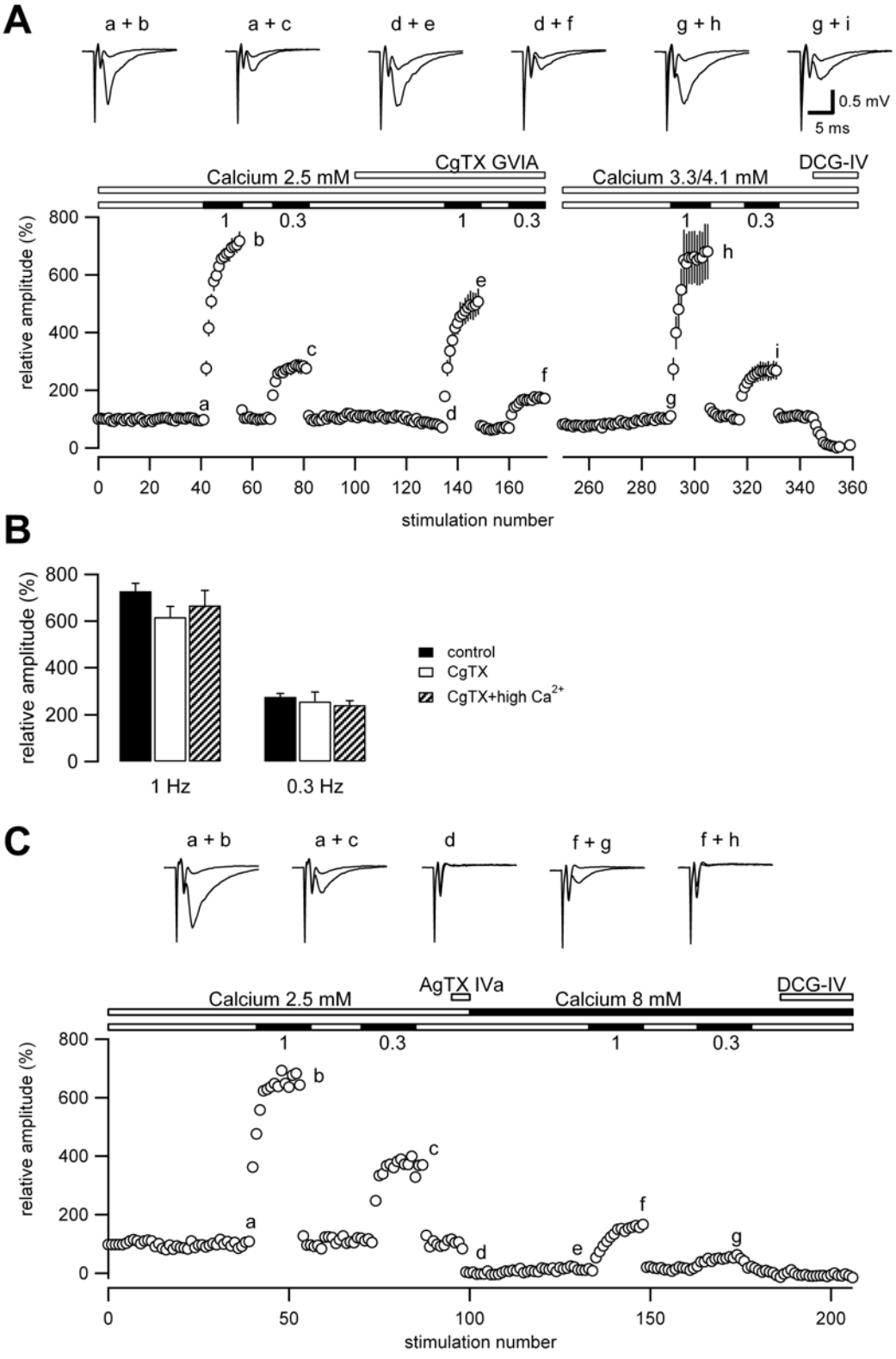

Figure 4.3: ***A role of voltage gated Ca^{2+} channels in frequency facilitation.*** **A** To test the role of N-type Ca^{2+}channels in MF-CA3 frequency facilitation, we bath applied the specific N-type channel blocker ω-conotoxin GVIa (CgTx GVIa, 2 μM). To correct for changes in the release probability caused by the reduced Ca^{2+} influx, we increased the extracellular Ca^{2+} concentration until we yield MF-fEPSP amplitudes equal to the conditions before application of the toxin. The time course of MF-fEPSP amplitudes is illustrated in the **lower** panel. **Middle** depicts the stimulation pattern indicate by numerals (in Hz), the durations of bath application of the compounds, and the Ca^{2+} concentration in the bath solution. Sample traces in the **upper** panel are taken from the time points indicated by the lowercase letters in the lower panel. Applying the toxin slightly reduced the size of MF-fEPSPs. Increasing the Ca^{2+} concentration recovered MF-fEPSP amplitudes to initial values. **B** Quantification of the amount of frequency facilitation after 15 stimulations at 1 Hz (**left**) and 0.3 Hz (**right**) revealed similar amounts of frequency facilitation for control (black bar), CgTX GVIa (white bar), and CgTX GVIa + high Ca^{2+} (hatched bar). **C** The selective P/Q-type channel blocker agatoxin IVa (AgTX IVa, 200 nM) was bath applied to hippocampal slices to determine the influence of P/Q-type channels on MF frequency facilitation. Illustration analogue to A (here a single experiment). The application of the toxin dramatically reduced the size of MF-fEPSPs that precluded a quantitative analysis of frequency facilitation. Even increasing the Ca^{2+} concentration to 8 mM only partially recovered MF-fEPSP amplitudes. Although a quantification of frequency facilitation was only possible in two experiment, all experiments showed pronounced frequency facilitation at 1 Hz and 0.3 Hz.

4.3.2 Blocking N-type Ca^{2+} channels in combination with application of low affinity Ca^{2+} buffers

In the preceding experiments we tested for a differential contribution of N- and P/Q-type Ca^{2+} channels to MF-CA3 frequency facilitation. The negative result of theses experiments might be explained, if both channels are located close together at an active zone. A consequence of this condition would be, that Ca^{2+} ions entering a mossy fiber synaptic terminal through one channel sybtype, e.g. N-type channels, can induce frequency facilitation, even if the Ca^{2+} sensor for frequency facilitation is located at the other Ca^{2+} channel subtype, e.g. P/Q-type channels.

Therefore, we performed a set of experiments, where we applied ω-conotoxin GVIa (2 μM) to block N-type Ca^{2+} channels in combination with the membrane perme-

able slow Ca^{2+} buffer EGTA-AM (100 μM), that precludes a spillover of Ca^{2+} ions entering through P/Q-type channels.
The combined application of EGTA-AM and ω-conotoxin GVIa reduced MF-fEPSP amplitudes to similar extends as seen in the previous experiments (see Fig.4.3A) (68.1 % ± 5.3 %, of baseline condition, n = 5, Fig.4.4A). Increasing the extracellular Ca^{2+} concentration to 3.3 or 4.1 mM Ca^{2+} recovered MF-fEPSP amplitudes to initial values (109.6 % ± 11.9 %, n = 5, Fig.4.4A). Under these circumstances neither 1 Hz (control: 529.6 % ± 53.0 %, n = 5, Fig.4.4A and black bar in Fig.4.4B, ω-conotoxin + EGTA-AM: 576.4 % ± 74.0 %, n = 5, Fig.4.4A and white bar in B, high Ca^{2+} + conotoxin + EGTA-AM: 418.7 % ± 50.1 %, n = 5, Fig.4.4A and hatched bar in B), nor 0.3 Hz facilitation (control: 232.1 % ± 22.8 %, n = 5, Fig.4.4A and black bar in Fig.4.4B, ω-conotoxin + EGTA-AM: 225.4 % ± 18.5 %, n = 5, Fig.4.4A and white bar in B, high Ca^{2+} + conotoxin + EGTA-AM: 195.4 % ± 15.3 %, n = 5, Fig.4.4A and hatched bar in B) showed significant changes in the amount of frequency facilitation.

We therefore concluded, that both voltage gated Ca^{2+} channel subtypes contribute equally to the expression of frequency facilitation at MF-CA3 synapses.

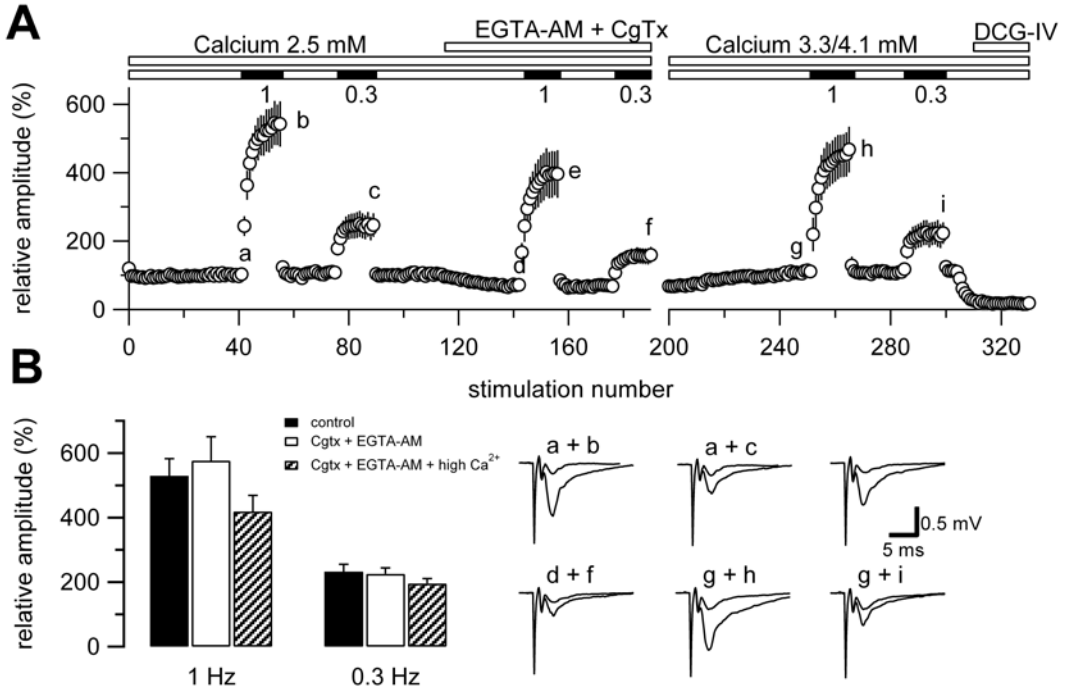

Figure 4.4: ***Combined application of ω-conotoxin and EGTA-AM does not influence frequency facilitation.*** **A** To test a scenario in which N-type and P/Q-type channels are colocated at MF-CA3 synapses we applied the specific N-type channel blocker ω-conotoxin GVIa (ω-CgTX GVIa, 2 μM) and the low affinity Ca^{2+} buffer EGTA-AM (100 μM) in combination. The time course of MF-fEPSP amplitudes is illustrated in the **lower** panel. **Middle** depicts the stimulation pattern indicate by numerals (in Hz), the durations of bath application of the compounds, and the Ca^{2+} concentration in the bath solution. Applying the toxin slightly reduced the size of MF-fEPSPs. Increasing the Ca^{2+} concentration recovered MF-fEPSP amplitudes to initial values. **B** Quantification of the amount of frequency facilitation after 15 stimulations at 1 Hz (**left**) and 0.3 Hz (**right**) revealed equal levels of frequency facilitation for control (black bar), CgTX GVIa (white bar), and CgTX GVIa with high Ca^{2+} (hatched bar). Sample traces on the right are obtained at the time points indicated by the lowercase letters in A.

4.4 Synaptic transmission at MF-CA3 synapses requires cooperative binding of Ca^{2+} ions

To quantify the Ca^{2+} dependence of synaptic transmission at MF-CA3 synapses, we systematically varied the extracellular Ca^{2+} (Ca_{ext}). We applied Ca_{ext} ranging from

1 mM to 2.5 mM (Fig.4.6A). With the following formula we calculated the relative intracellular peak Ca^{2+} microdomain concentration (Ca_{int}):

$$Ca_{int} = 0.85 \times \frac{2.7 \times Ca_{ext}}{Ca_{ext} + 3.3} \tag{4.1}$$

Table 4.5 shows the results of this conversion.

Ca_{ext} (mM)	Ca_{int} (mM)	normalized Ca_{int} (mM)
10.0	2.03	1.74
5.00	1.61	1.40
3.30	1.35	1.16
2.50	1.16	1.00
2.00	1.02	0.88
1.50	0.84	0.73
1.00	0.63	0.54
0.90	0.58	0.50

Figure 4.5: ***Conversion of*** Ca_{ext} ***into*** Ca_{int} This table depicts different Ca_{ext} with their corresponding Ca_{int}, and the normalized Ca_{int} (normalized to 2.5 mM Ca_{ext}).

We could observe a non-linear correlation between the MF-fEPSP amplitudes and Ca_{int}. Similar observations have previously been made at various types of synapses (Bollmann et al., 2000; Dodge and Rahamimoff, 1967; Neher and Sakaba, 2001). Cooperative binding of Ca^{2+} ions at the Ca^{2+} sensor molecule responsible for transmitter release has been suggested to be responsible for this finding.

To determine the level of cooperativity of transmitter release (n) we used the linearization method with a Hill-diagram[1]. Therefore, we normalized the MF-fEPSP amplitudes and Ca_{int} to the values at 2.5 mM Ca_{ext} (Table 4.5). We plotted these values in a Hill-diagram in a double logarithmic plot (Fig.4.6A_2). The gradient at

[1]Enzymkinetik. Theorie und Methoden, Vol.3, 2000 by Hans Bisswanger, Wiley-VCH

zero equals the Hill-coefficient and gives an approximation of n. To determine this gradient we used a linear regression:

$$log_{(release)} = n \times log_{(Ca_{int})} \tag{4.2}$$

When we fitted our data with this function this yielded $n = 3.6$. This is a value quite similar to those reported for the neuromuscular junction (Dodge and Rahamimoff, 1967) or the Calyx of Held (Bollmann et al., 2000; Neher and Sakaba, 2001).

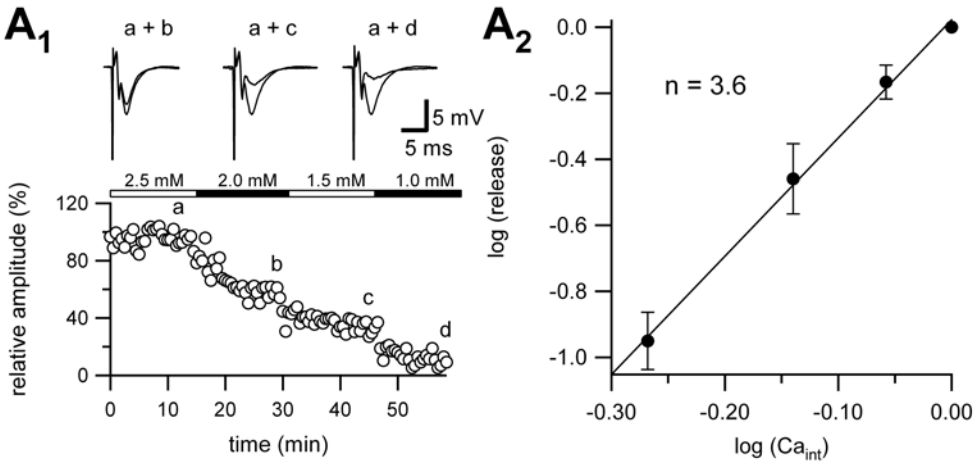

Figure 4.6: ***Synaptic transmission at the MF-CA3 synapse is cooperative.*** $\mathbf{A}_1$ To investigate the dependence of synaptic transmission from the Ca^{2+} concentration we varied the extracellular Ca^{2+} concentration stepwise from 2.5 to 1.0 mM. The **lower** panel illustrates the time course of MF-fEPSP amplitudes of an example experiment at the different Ca^{2+} concentrations that are indicated by white and black bars in the **middle**. Sample traces in the **upper** panel are obtained at the time points indicated by the lowercase letters. MF-fEPSP amplitudes declined non-linearly with decreasing Ca^{2+} concentrations. $\mathbf{A}_2$ From these experiments we quantified the Ca^{2+} dependence of synaptic transmission at the MF-CA3 synapse. Shown are values for MF-fEPSP amplitudes and Ca_{int} in a double logarithmic plot. A linear regression yielded a gradient of n = 3.6.

4.5 The Ca^{2+} dependence of MF-CA3 frequency facilitation

To our knowledge, it has never formally been shown that Ca^{2+} influx is underlying frequency facilitation at MF-CA3 synapses. To test for a dependence of frequency facilitation on Ca^{2+}, we measured frequency facilitation at different Ca_{ext} (0.9, 1.5, 2.5, 3.3, 5.0, and 10.0 mM; for conversion into Ca_{int} see Table 4.5).

Comparing frequency facilitation at the different Ca_{int} revealed a complex relationship (Fig.4.7). To explain the relationship between frequency facilitation and Ca_{int} we choose representative for the early phase of facilitation the ratio of the 2^{nd} fEPSP amplitude to the 1^{st} of a 15 stimulation train (Fig.4.7B_1) and representative for the late phase of facilitation the ratio of the 15^{th} fEPSP amplitude to the first (Fig.4.7B_2).
At the beginning of a facilitation train the amount of facilitation increased with increasing Ca_{int}. In contrast, at later points in a train which achieve high levels of frequency facilitation the magnitude of facilitation decreased with increasing Ca_{int}. The intermediate pulses (3^{rd}, 5^{th}, and 10th) showed intermediate Ca_{int} dependencies (Fig.4.7B_3).

We also analyzed frequency facilitation at 0.3 Hz, because at this frequency the amount of facilitation is smaller than at 1 Hz and therefore might show a differential dependence on Ca_{int}. For the 2^{nd} pulse a similar relationship as at 1 Hz became obvious (Fig.4.7D_1). Moreover, MF-fEPSPs at 0.3 Hz behave in their dependence on Ca_{int} similarly to the MF-fEPSPs at 1 Hz resulting in the same amounts of facilitation, although if the amount of facilitation was reached at a different stimulation pulse (Fig.4.7D_1 - D_3).

In summary, these experiments showed that frequency facilitation at MF-CA3 synapses indeed depends on the influx of Ca^{2+} ions. Facilitation at 1 Hz and 0.3 Hz was not differentially influenced by the Ca^{2+} concentration suggesting a similar mechanism underlying both.

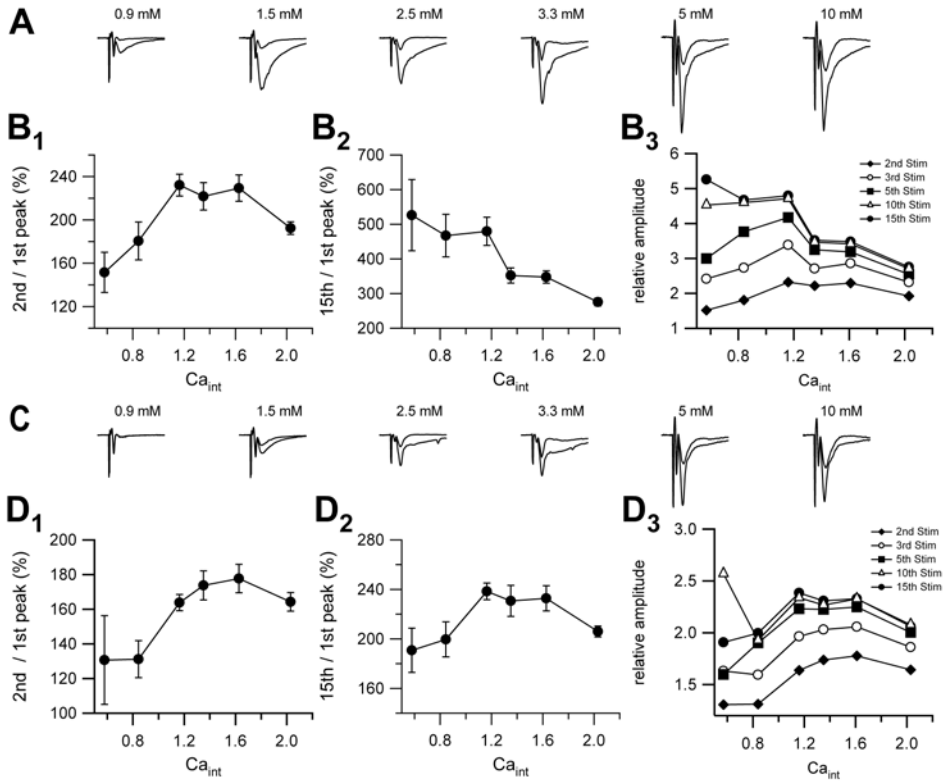

Figure 4.7: ***Dependence of frequency facilitation from the intracellular Ca^{2+} concentration.*** **A** Overlay of sample traces at 0.025 Hz and 1 Hz after 15 stimulations under different extracellular Ca^{2+} concentrations. $\mathbf{B}_1$ Shown are MF-fEPSP amplitudes for the 2^{nd} stimulation in a 1 Hz stimulation train in dependence on Ca_{int}. $\mathbf{B}_2$ same as B_1, but shown are MF-fEPSP amplitudes for the 15^{th} stimulation. $\mathbf{B}_3$ illustrates the MF-fEPSP amplitudes for the 2^{nd}, 3^{rd}, 5^{th}, 10^{th}, and 15^{th} stimulation. Note that error bars are removed. When high levels of frequency facilitation were attained, such as when looking at the 15^{th} stimulus, the amount of frequency facilitation declined with increasing Ca_{int}. At lower facilitation levels, as obtained by looking at the 2^{nd} stimulus in a train, initially frequency facilitation increased with higher Ca_{int}, but start to depress at high Ca_{int}. Facilitation at other stimuli showed an intermediate behaviour in dependence on Ca_{int}. **C** same as B but at 0.3 Hz stimulation frequency. $\mathbf{D}_1$-$\mathbf{D}_3$ analog to B_1-B_3, but for 0.3 Hz stimulation trains. Whereas the dependence of the 2^{nd} stimulus in a train showed a similar behaviour as at 1 Hz, the dependence of the 15^{th} stimulus was different.

4.6 Modelling the Ca^{2+} dependence of MF-CA3 frequency facilitation

In order to explain this complex relationship between frequency facilitation and Ca_{int}, we tested different mathematical models for facilitation. Because of the high variability of the data obtained at 0.57 mM Ca_{ext} we excluded these data.
Although we could explain the occurrence of paired-pulse facilitation with a classical single sensor model (see appendix B), this model was insufficient to explain frequency facilitation.
We therefore developed a new model incorporating two distinct Ca^{2+} bindings sites. One of the binding sites is responsible for basal transmitter release (release sensor), whereas the second gives rise to frequency facilitation (frequency facilitation sensor) by altering the Ca^{2+} affinity of the first binding site. This would enhance the release probability during a facilitation train and cause a potentiation of transmitter release. Cooperative binding of Ca^{2+} ions at the release Ca^{2+} sensor causing a non-linear dependence of transmitter release can be described by the following equation:

$$release(Ca_{int}) = \frac{Ca_{int}^n}{Ca_{int}^n + Kd_{rel}^n} \tag{4.3}$$

Where Kd_{rel} is the relative Ca^{2+} affinity of the release sensor and n the level of cooperativity. The release during frequency facilitation is described by the following function:

$$release(Ca_{int}) = \frac{Ca_{int}^n}{Ca_{int}^n + (1 - b \times Kd_{rel})^n} \tag{4.4}$$

Where 1 - b (b $<$ 1) represents a stimulus dependent increase in Ca^{2+} affinity. To yield the relative amount of frequency facilitation we divide equation 4.4 by equation 4.3:

$$release(Ca_{int}) = \frac{Ca_{int}^n + Kd_{rel}^n}{Ca_{int}^n + (1 - b \times Kd_{rel})^n} \tag{4.5}$$

We now introduce *occ*, that denotes the occupancy of the Ca^{2+} binding site of the frequency facilitation sensor and replaces *b*. We also introduce *coup*, which is a proportionality constant:

$$release(Ca_{int}) = \frac{Ca_{int}^n + Kd_{rel}^n}{Ca_{int}^n + ((1 - occ \times coup) \times Kd_{rel})^n} \tag{4.6}$$

Our model assumes that the occupancy of the Ca^{2+} binding site of the frequency facilitation sensor increases during a facilitation train. Therefore, *occ* is a recursive function describing this increase of occupancy during a facilitation train:

$$occ_i = (occ(i-1) + (A - occ(i-1)) \times rf) \times df \tag{4.7}$$

$$df = e^{-ISI \times K_{off}} \tag{4.8}$$

$$rf = 1 - e^{-D \times (Ca_{int} \times K_{on} + K_{off})} \tag{4.9}$$

Where ISI is the interstimulus interval, i the stimulus number, rf the number of binding sites that would be occupied by an infinite long Ca^{2+} influx, K_{off} the rate at which Ca^{2+} unbinds from the binding site, and Kd_{FF} the relative Ca^{2+} affinity of the frequency facilitation sensor. D stands for the duration of Ca^{2+} influx, usually determined by the duration of an action potential.

We tested two different models for Ca^{2+} binding at the frequency facilitation sensor:

$$A = \frac{Ca_{int}}{Ca_{int} + Kd_{FF}} \tag{4.10}$$

describes non-cooperative binding at the frequency facilitation sensor, whereas

$$A = \frac{{Ca_{int}}^m}{{Ca_{int}}^m + {Kd_{FF}}^m} \tag{4.11}$$

simulates cooperative binding at this sensor with the cooperativity level m.

In the first step we used equation 4.6 to fit simultaneously the data sets for 1 Hz and 0.3 Hz with the non-cooperative model. The cooperativity value for the release sensor $n = 3.6$ was obtained from the linear regression in Fig.4.6B. The values for ISI were determined by the stimulation frequency (1 Hz: $ISI = 1$ s, 0.3 Hz: $ISI = 3.3$ s). This fitting procedure resulted in unphysiological values for the model parameters.

Therefore, we rejected this model and introduced cooperative binding of Ca^{2+} ions at the frequency facilitation sensor. Results of fitting the data sets for 1 Hz and 0.3 Hz simultaneously with this model are shown in Fig.4.8A_1 - A_3 for 0.3 Hz and B_2 - B_3 for 1 Hz.

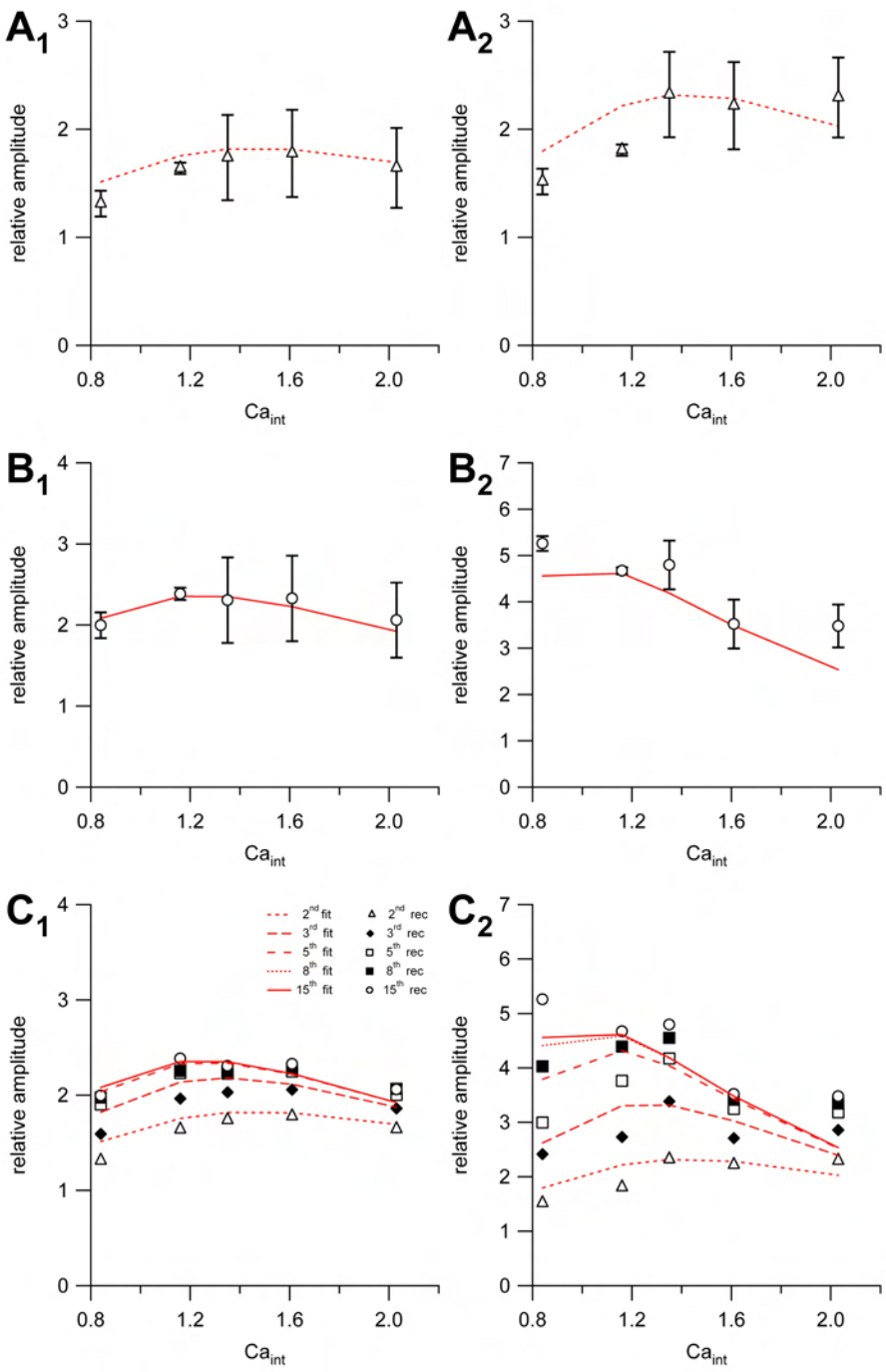

Figure 4.8: ***Predictions of the model.*** $\mathbf{A}_1$ Overlay of MF-fEPSP amplitudes at the 2^{nd} stimulation of a facilitation train at 0.3 Hz with the predictions of the cooperative model (dotted line in red). $\mathbf{A}_2$ same for 1 Hz. $\mathbf{B}_1$ and $\mathbf{B}_2$ same as A but for the 15^{th} stimulation. Predictions of the model are indicated by the red lines. $\mathbf{C}_1$ and $\mathbf{C}_2$ illustrates the MF-fEPSP amplitudes at 0.3 Hz (C_1) and 1 Hz (C_2) for the 2^{nd}, 3^{rd}, 5^{th}, 8^{th}, and 15^{th} stimulation with the predictions of the model (red lines). Note that error bars are removed.

From the superimposed data curves in Fig.4.8A_1 - A_3 and B_2 - B_3 it becomes obvious, that the model approximates the recorded data. At early stimulations the data are not accurately described by the model. In these situations the model predicts more facilitation than we observed in the recordings.

Nevertheless, the model shows that Ca^{2+} binding to two different Ca^{2+} sensors at the release site of a mossy fiber presynaptic terminal can be used to explain MF-CA3 frequency facilitation. A low affinity binding site mediates transmitter release under baseline conditions and a second high affinity Ca^{2+} sensor is responsible for the facilitation of synaptic transmission during repetitive stimulations.

4.7 Saturation of frequency facilitation at MF-CA3 synapses is not caused by depletion of the RRP

During a frequency facilitation train we could observe an early phase of facilitation, in which fEPSP are rapidly potentiated, and a subsequent phase, in which the potentiation saturated. We therefore asked, what is causing this saturation?

Because of its small size, the RRP would be rapidly depleted during repetitive stimulations. Therefore this pool has to be refilled to maintain transmitter release. At MF-CA3 synapses a major source for refilling of the RRP is the reserve-releasable pool (Suyama et al., 2007). This refilling of the RRP by the reserve-releasable pool is a time consuming process, because vesicles have to maturate before they become part of the RRP. If the rate of transmitter release is higher than the refilling rate, the refilling rate would limit the maximum amount of transmitter release. The contribution of this mechanism to saturation of facilitation should depend on the release probability, i.e. under situations of high release probability more vesicles are released by a single stimulation and depletion of the RRP should occur faster.

To investigate this issue, we compared facilitation at different release probabilities. We measured paired-pulse facilitation at different extracellular Ca^{2+} concentrations, because the release probability depends on the Ca^{2+} concentration (Sakaba and Neher, 2001; Schneggenburger and Neher, 2000).
MF-fEPSPs showed pronounced paired-pulse facilitation at low Ca^{2+} concentration. This facilitation decreased with increasing ISIs (10 ms: 326.9 % ± 25.3 %; 500 ms: 141.9 % ± 11.4 % Fig.4.9B filled circles). At high Ca^{2+} concentrations and short ISIs (< 40 ms) paired-pulse facilitation was smaller compared to low Ca^{2+} concentration. This indicates a contribution of vesicle depletion at these ISIs. At longer ISIs the difference in paired-pulse facilitation between low and high Ca^{2+} concentration was no longer visible (10 ms ISI: 147.2 % ± 11.0 %; 500 ms: 153.5 % ± 4.4 %, n = 4, Fig.4.9B open circles).

Taken together, there was a differential behavior of paired-pulse facilitation under low and high Ca^{2+} concentration at short ISIs. We concluded that vesicle depletion might limit the amount of facilitation at these rather small ISIs. In contrast, there was no obvious difference in the paired-pulse ratios at ISIs > 40 ms. Therefore, at ISIs > 40 ms there is no contribution of vesicle depletion to facilitation. Finally, we can reject the hypothesis that saturation of frequency facilitation at 0.3 or 1 Hz is caused by depletion of the RRP.

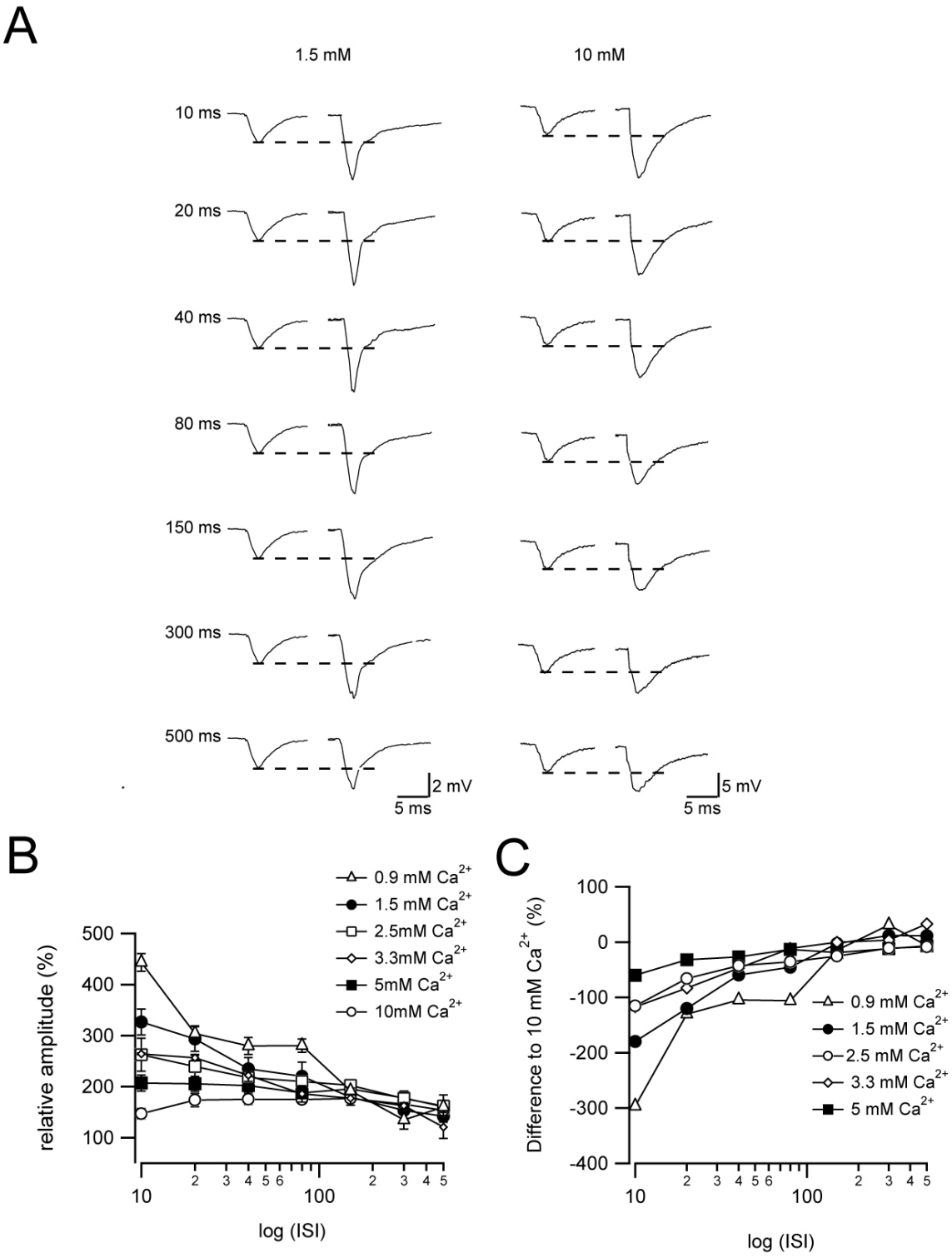

Figure 4.9: ***Is saturation of facilitation due to replenishment of the RRP?***. **A** Representative MF-fEPSP sample traces at ISIs ranging from 10 to 500 ms at 1.5 mM (**left**) and 10 mM (**right**) extracellular Ca^{2+} concentration. Note that the fiber volley and the stimulation artefact have been removed from the traces. **B** illustrates the amount of paired-pulse facilitation at

different ISIs and different Ca^{2+} concentrations. At short ISIs there is an obvious difference in the level of paired-pulse facilitation that declines with longer intervals. **C** To have a better estimate of the contribution of vesicle replenishment to facilitation we plotted the amount of paired-pulse facilitation as the difference to the data obtained at 10 mM Ca^{2+}. In this illustration it becomes obvious that at ISIs > 40 ms vesicle replenishment can no longer contribute to facilitation, because the amount of paired-pulse facilitation is equal in all conditions.

4.8 Frequency facilitation is independent of common presynaptic signalling pathways

Finally, we tested if there is a contribution of presynaptic signalling pathways to frequency facilitation at MF-CA3 synapses. First, we investigated a possible involvement of αCamKII to frequency facilitation, because αCamKII has been reported to influence frequency facilitation at MF-CA3 synapses (Salin et al., 1996).

Therefore, we tested the specific CamKII antagonist KN-62 (3.5 μM) on its ability to influence frequency facilitation at the MF-CA3 synapse.
Frequency facilitation was not altered by application of the inhibitor at 1 Hz (621.0 % ± 90.6 % to 551.6 % ± 59.2 %) and 0.3 Hz (277.3 % ± 17.2 % to 268.8 % ± 21.3 %, n = 4, Fig.4.10A_1 and A_2). In addition, application of another specific CamKII antagonist (KN-93, 10 μM) left frequency facilitation at 1 Hz unaffected (425.9 % ± 71.7 % to 502.5 % ± 60.9 %, Fig.4.10A_2).
We further examined frequency facilitation in αCamKII knock-out mice . Frequency facilitation appeared unaltered in these knock-out mice compared to littermate controls (1 Hz: 490.3 % ± 7.7 % to 426.8 % ± 21.0 %, n = 5; 0.3 Hz: 263.4% ± 8.5 % to 262.5 % ± 3.8 %, n = 4, Fig.4.10B).
In conclusion, we think that the activation of αCamKII is not necessary for frequency facilitation at MF-CA3 synapses.

Using the same experimental design we tested the influence of different other presynaptic signalling cascades on their contribution to frequency facilitation at MF-CA3

synapses. Beside αCamKII, there are other protein kinases known to phosphorylate synapsins in a Ca^{2+} dependent manner (for review: Hilfiker et al., 1999). Phosphorylation of synapsin by PKA and MAPK both lead to a reduced affinity of synapsin to attach synaptic vesicles to cytosceletal elements.
To test for a possible involvement of MAPK signalling in frequency facilitation at MF-CA3 synapses we bath applied the specific MAPK antagonists UO126 (20 μM, n = 4, Fig.4.10C_1 and C_2) and PD98056 (50 μM, n = 3, Fig.4.10C_2). In these experiments we found no influence on frequency facilitation by application of the blockers. Facilitation was unaltered following application of either UO126 (1 Hz: 744.1 % ± 114.4 % to 727.6 % ± 83.5 %, 0.3 Hz: 558.3 % ± 103.4 % to 493.8 % ± 82.8 %) or PD98056 (1 Hz: 900.9 % ± 301.4 % to 733.5 % ± 190.0 %, 0.3 Hz 542.7 % ± 227.0 % to 474.6 % ± 170.1 %).

Furthermore, we applied the cAMP analog Rp-cAMPs (100 μM, n = 2, Fig.4.10D_1 and D_2), which is a competitive inhibitor of PKA. We found frequency facilitation unchanged (1 Hz: 997.8 % ± 104.6 % to 867.1 % ± 60.5 %, 0.3 Hz: 377.3 % ± 21.5 % to 395.0 % ± 15.4 %).
Further experiments with the protein kinase C (PKC) blocker staurosporin (200 nM, n = 3, Fig.4.10D_1 and D_2) revealed that frequency facilitation at MF-CA3 synapses is also independent of activity of this kinase (1 Hz: 933.9 % ± 172.2 % to 954.3 % ± 149.8 %, 0.3 Hz: 315.1 % ± 20.5 % to 343.0 % ± 55.6 %).

Protein function is not only influenced by phosphorylation, but could also be influenced by dephosphorylation. We tested for a possible involvement of protein phosphatases in regulating frequency facilitation and applied the specific inhibitor of the protein phosphatase calcineurin (PP2B) cyclosporin A (100 μM, n = 3, Fig.4.10D_1 and D_2), in combination with okadaic acid (25 μM), an inhibitor of phosphatase 1 and 2A. We found no change in frequency facilitation (1 Hz: 664.2 % ± 63.1 % to 508.5 % ± 46.4 %; 0.3 Hz 266.5 % ± 29.9 % to 245.9 % ± 21.0 %).

Because it was shown that synapsins regulate the availability of synaptic vesicles by interaction with elements of the cytoskeleton (Owe et al., 2009; Rosahl et al., 1993,

1995; Ryan et al., 1996), we tested the effect of different pharmacological agents that interfere with the integrity of the cytoskeleton.
We also found frequency facilitation unchanged after application of the microtubule depolymerising agent nocodazole (10 μM, n = 3, Fig.4.10D_1 and D_2, 1 Hz: 969.5 % ± 223.4 % to 797.9 % ± 147.4 %; 0.3 Hz: 383.8 % ± 74.3 % to 346.6 % ± 74.7 %), by application of the f-actin stabilizing compound jasplakinolide (200 nM, n = 4, Fig.4.10D_1 and D_2, 1 Hz: 787.9 % ± 49.5 % to 784.9 % ± 103.9 %, 0.3 Hz: 309.1 % ± 9.2 % to 327.6 % ± 30.4 %), and by application of the f-actin destabilizing agent latrunkulin A (5 μM, n = 4, Fig.4.10D_1 and D_2, 1 Hz: 726.7 % ± 43.1 % to 588.7 % ± 69.1 %; 0.3 Hz: 316.0 % ± 12.1 % to 287.0 % ± 42.1 %).

Another signalling pathway was shown to affect STP: The phosphatidyl-inositol (PI) pathway (Iino, 2006). We therefore applied the PI-4-kinase inhibitor Wortmannin (200 nM, n = 8, Fig.4.10D_1 and D_2). Furthermore, we applied wortmannin at 1 μM (n = 3, Fig.4.10B_1 and D_2), because at this concentration wortmannin also to blocks PI-3-kinase. At both concentrations we found no changes in frequency facilitation (200 nM, 1 Hz: 766.7 % ± 59.7 % to 591.9 % ± 51.0 %, 0.3 Hz: 337.9 % ± 24.7 % to 298.2 % ± 28.0 %, 1 μM, 1 Hz: 676.5 % ± 55.2 % to 889.8 % ± 113.2 %, 0.3 Hz: 322.8 % ± 24.6 % to 397.6 % ± 16.0 %).

Finally, we tested the role of KARs in MF-CA3 frequency facilitation. Therefore, we applied the specific KAR antagonist NS-102 (10 μM, n = 5, Fig.4.10D_1 and D_2), but found frequency facilitation unaffected (1 Hz: 636.3 % ± 54.6 % to 561.5 % ± 37.8 %, 0.3 Hz: 269.5 % ± 15.5 % to 261.8 % ± 10.8 %).

In summary, we found no influence of kinases or phosphatases on MF-CA3 frequency facilitation. Therefore we concluded, that MF-CA3 frequency facilitation is independent of common presynaptic signalling pathways. Moreover, this form of STP seems to be independent of the integrity of the cytoskeleton, KARs, and phosphatidyl-inositol signalling.
This is consistent with the idea of a more direct Ca^{2+}-dependent signalling pathway that does not involve activation of kinases or phosphatases.

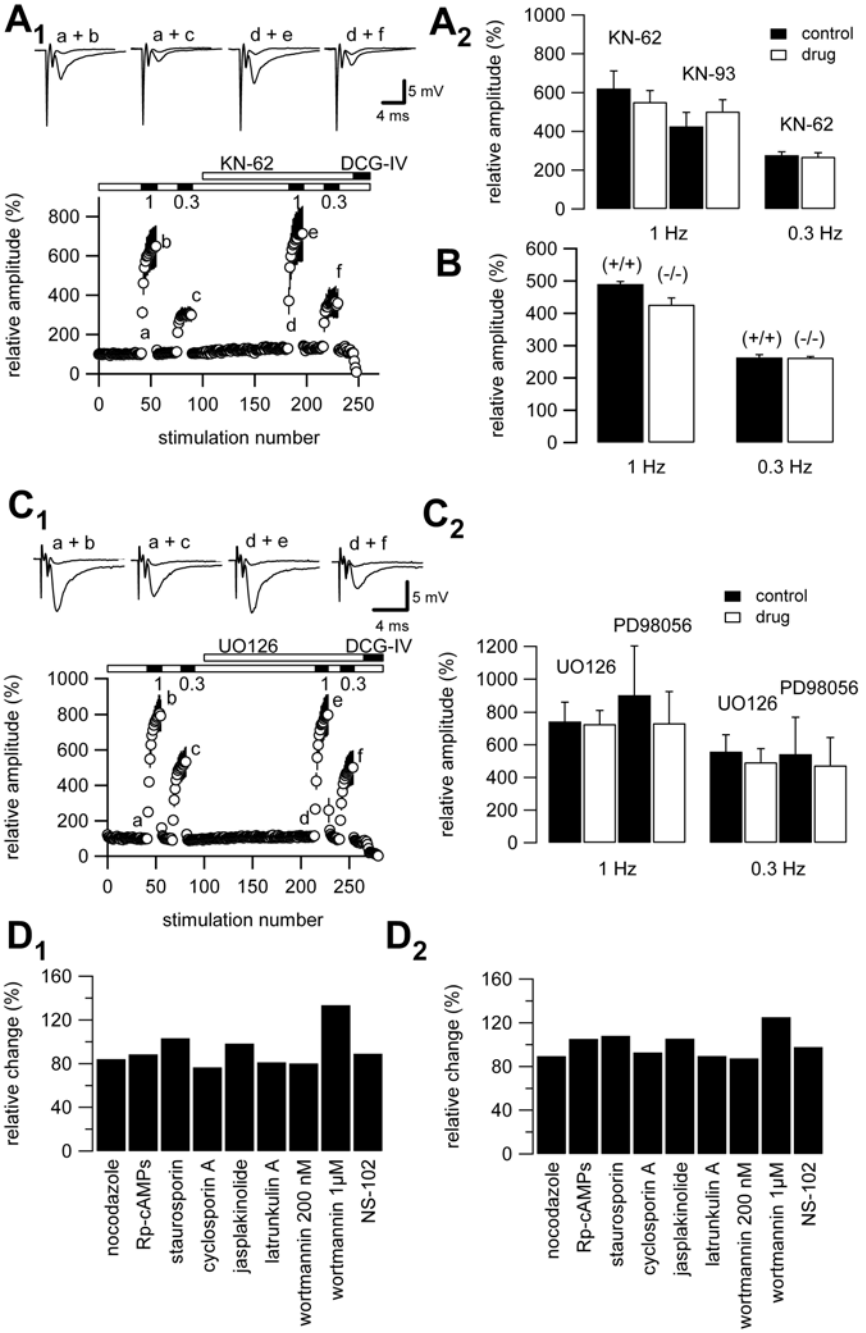

Figure 4.10: ***MF-CA3 frequency facilitation is independent of common intracellular signalling pathways.*** $\mathbf{A}_1$ Frequency facilitation is unaffected by application of blockers of CamKII. **Lower** illustrated the time course of MF-fEPSP amplitudes at different stimulation frequencies (**middle** indicated by numerals in Hz) before and after application of KN-62 (10 μM). **Upper** depicts representative sample traces taken at the time points indicated by the lowercase letters. $\mathbf{A}_2$ Quantification of the level of frequency facilitation after 15 stimulations at 1 Hz (**left**)

and 0.3 Hz (**right**) before (black bars) and after (white bars) application of KN-62 and KN-93 (3.5 μM). The amount of frequency facilitation was not affected by the two blockers. **B** We investigated frequency facilitation in αCamKII null mutants ((-/-), white bars) and compared them to littermate controls ((+/+), black bars). We observed equal amounts of frequency facilitation at 1 Hz (**right**) and 0.3 Hz (**left**). $\mathbf{C}_1$ Illustration analogue to A1, but for application of the selective MAPK inhibitor UO126 (20 μM). The levels of frequency facilitation were comparable before and after application of the inhibitor. $\mathbf{C}_2$ Summary of the magnitude of frequency facilitation at 1 Hz (**left**) and 0.3 Hz (**right**) for the application of UO126 and another specific blocker of the MAPK (PD98056, 50 μM) before (black bar) and after (white bar) application of the blockers. Application of inhibitors of MAPK had no influence on frequency facilitation. In analog experiments we investigated the role of other presynaptic, Ca^{2+} activated signalling pathways: nocodazole (10 μM), Rp-cAMPs (100 μM), staurosporin (200 nM), cyclosporin (200 μM), jasplakinolide (200 nM), latrunkulin A (5 μM), wortmannin (200 nM and 1 μM), U73122 (20 μM), and NS-102 (10 μM). The results expressed as the ratio of frequency facilitation before and after application of the compounds are shown for 1 Hz in (D_1) and for 0.3 Hz in (D_2). Frequency facilitation was equal in all conditions.

Chapter 5

Discussion

In the last years, different mechanisms have been proposed to underlie frequency facilitation at MF-CA3 synapses. The available literature about frequency facilitation is controversial, because different groups favor different induction mechanisms (Blatow et al., 2003; Breustedt and Schmitz, 2004; Contractor et al., 2001; Kamiya et al., 2002; Kukley et al., 2005; Kwon and Castillo, 2008; Lauri et al., 2003; Moore et al., 2003; Salin et al., 1996; Schmitz et al., 2001).

The influx of Ca^{2+} ions into presynaptic terminals is responsible for basal transmitter release (Dodge and Rahamimoff, 1967; Katz and Miledi, 1967; Miledi, 1973; Rahamimoff and Dodge, 1969) and has been proposed to underlie the induction of multiple forms of short-term synaptic plasticity (for review: Zucker and Regehr, 2002).
Moreover, the accumulation of bulk Ca^{2+} in a presynaptic terminal has been shown to underlie facilitation at the neuromuscular junction (Katz and Miledi, 1968) and the squid giant synapse (Zucker and Stockbridge, 1983). This accumulation occurs, if Ca^{2+} ions from prior stimulations are not completely removed from the synaptic terminal before the next action potential arrives.
In contrast, it has been shown that bulk Ca^{2+} concentrations reach resting levels already after several seconds (Shimizu et al., 2008). Because frequency facilitation

can even be induced at rather low stimulation frequencies (0.1 - 10 Hz)(Salin et al., 1996), an accumulation of bulk Ca^{2+} is most unlikely to underlie frequency facilitation at MF-CA3 synapses.

But if a persistent increase of bulk Ca^{2+} is not responsible for facilitation at the MF-CA3 synapse, what could be an alternative mechanism?

A different explanation of the residual Ca^{2+} hypothesis (Katz and Miledi, 1968) is that not an accumulation of bulk Ca^{2+} leads to facilitation of transmitter release, but slow unbinding of Ca^{2+} ions from the Ca^{2+} binding site of the sensor responsible for baseline synaptic transmission (Zucker and Regehr, 2002).

Therefore, we tested if a classical single site model (adapted from: Dobrunz and Stevens, 1997) can explain facilitation at MF-CA3 synapses. This model explained paired-pulse facilitation (see Appendix B), but not frequency facilitation at MF-CA3 synapses.

Alternatively, facilitation could be induced by Ca^{2+} binding to a different Ca^{2+} binding site (Delaney et al., 1989; Swandulla et al., 1991). Kamiya and Zucker (1994) suggested that the time course of facilitation at the crayfish neuromuscular junction is determined by the time course of bulk Ca^{2+} acting on a second binding site. In contrast, other groups proposed that facilitation is a consequence of slow Ca^{2+} unbinding from the second binding site (Blundon et al., 1993; Winslow et al., 1994).

It has been shown that two forms of transmitter release, synchronous and asynchronous release, are mediated by two different Ca^{2+} sensor molecules (Goda and Stevens, 1994). Therefore, the existence of a second Ca^{2+} binding site that mediates frequency facilitation is not unlikely.

Although most unlikely, we tested the hypothesis that frequency facilitation at the MF-CA3 synapse is induced by an accumulation of presynaptic bulk Ca^{2+}.

Therefore, we recorded frequency and paired-pulse facilitation in the presence of the low affinity Ca^{2+} buffer EGTA-AM (100 μM). Because of the low affinity, this buffer interferes with bulk Ca^{2+} signalling (Adler et al., 1991; Cummings et al., 1996), but leaves Ca^{2+} microdomains unaffected.

After application of EGTA-AM we observed a potent reduction of paired-pulse facilitation at CA3-CA1 synapses but not at MF-CA3 synapses. Similar results have previously been reported (Blatow et al., 2003). In contrast, Castillo et al. (1996) could show by application of 200 μM EGTA-AM that synaptic transmission and paired-pulse facilitation at MF-CA3 synapses is strongly reduced following application of EGTA-AM.

The higher concentration of EGTA-AM used by Castillo et al. (1996) could account in part for the divergence. Interestingly, Castillo et al. (1996) show a reduction of paired-pulse facilitation but do not quantify their results. The reduction of baseline transmission reported by Castillo et al. (1996) could have caused a worse signal-to-noise ratio in their recordings. Moreover, this could have prevented a quantification of the results. Therefore we guess, that the reduction of paired-pulse facilitation shown by Castillo et al. (1996) is an artificial secondary effect of the reduced baseline transmission.

But why blocks EGTA-AM paired-pulse facilitation at Schaffer-collaterals and not on mossy fibers?

Although EGTA-AM is a membrane permeable molecule that is not actively transported, there could be a preferential accumulation of EGTA in terminals of the Schaffer-collateral pathway. We could find no evidence for such a preferential import of EGTA-AM into different types of synaptic terminals in the literature.

In conclusion, our experiments with EGTA-AM favor the idea, that a persistent increase of bulk Ca^{2+} during repetitive stimulations cannot explain facilitation at MF-CA3 synapses. This makes the idea most likely, that the Ca^{2+} sensor for facilitation is located within the range of Ca^{2+} microdomains.

Therefore, we tested if this sensor is predominantly located near a certain voltage gated Ca^{2+} channel subtype. Mossy fiber boutons have been shown to express three different types of voltage gated Ca^{2+} channels: N-, P/Q-, and R-type channels (Castillo et al., 1996, 1994; Dietrich et al., 2003). An involvement of R-type channels in frequency facilitation has been excluded by Dietrich et al. (2003). Therefore, we

tested the role of N- and P/Q-type channels.

Blocking one Ca^{2+} channel subtype will leave synapses with Ca^{2+} influx through the remaining channel subtypes. This will lead to a reduction of the overall Ca^{2+} influx at the presynapse. Because the transmitter release depends on the presynaptic Ca^{2+} concentration (Sakaba and Neher, 2001; Schneggenburger and Neher, 2000), this will reduce the amount of transmitter release. This effect can be countered by increasing the Ca^{2+} influx through the remaining channels, i.e. by increasing the extracellular Ca^{2+} concentration.

Applying the selective N-type channel blocker ω-conotoxin GVIa (2 μM) caused a reduction of the fEPSP amplitudes of about 25 %. Similar experiments performed by Castillo et al. (1994) with guinea pigs showed that synaptic transmission at MF-CA3 synapses is reduced by up to 75 % after application of 1 μM ω-conotoxin GVIa. Although we could rescue synaptic transmission by increasing the bath Ca^{2+} concentration to 3.3 or 4.1 mM, we were not able to observe any changes in frequency facilitation.

Application of the selective P/Q-type channel blocker agatoxin IVa completely blocked synaptic transmission. Consistent with our results, Castillo et al. (1994) found a dramatic decrease of MF-CA3 synaptic responses after application of agatoxin IVa (1 μM). Increasing the bath Ca^{2+} concentration to 8 mM failed to rescue the complete MF-CA3 synaptic transmission in all experiments. In the experiment, where we observed a potent although still incomplete recovery of fEPSP amplitudes, frequency facilitation was unchanged. We cannot exclude that the incomplete recovery occluded a possible reduction of frequency facilitation.

Why is there a smaller block of synaptic transmission following application of ω-conotoxin GVIa in our experiments compared to Castillo et al. (1994)?

There seems to be a differential contribution of P/Q- and N-type channels to MF-CA3 synaptic transmission across species. At the mouse MF-CA3 synapse transmission is predominately mediated by Ca^{2+} influx through P/Q-type channels with a minor contribution of N-type channels, whereas in guinea pigs there is a larger contribution of N-type channels.

There is no appropriate data available about the exact distribution of P/Q- and N-type channels across the presynaptic membrane of a MF-CA3 synapse. A colocalization of both channel subtypes is possible. In this situation, the Ca^{2+} sensor can be located near a P/Q-type channel, but is also accessible by spillover of Ca^{2+} ions entering through N-type channels, and vice versa. To test such scenario we coapplied ω-conotoxin GVIa (2 μM) to block N-type channels with EGTA-AM (100 μM) to block the spillover of Ca^{2+} ions from P/Q-type channels. In these experiments frequency facilitation was also unchanged.
These experiments make it most likely, that Ca^{2+} ions entering through P/Q- and N-type channels can equally access the Ca^{2+} sensor responsible for the induction of frequency facilitation.

Synaptic transmission in the CNS and at the neuromuscular junction requires cooperative binding of Ca^{2+} ions at a Ca^{2+} binding site (Dodge and Rahamimoff, 1967; Rahamimoff and Dodge, 1969; Schneggenburger and Neher, 2000).
We measured fEPSPs at different extracellular Ca^{2+} concentrations to determine the cooperativity at the MF-CA3 synapse. Afterwards, we quantified the level of cooperativity with the linearization method with a Hill-plot. In this diagram the gradient at zero equals the Hill-coefficient (n), and moreover, the number of ions that have to bind at the binding site to induce transmitter release. Although this method usually underestimates the level of cooperativity (Reid et al., 2003), it is widely used to determine cooperativity of enzymatic activity[1]. We estimated $n = 3.6$, which is in agreement with findings at other synapses (Bollmann et al., 2000; Sakaba and Neher, 2001; Schneggenburger and Neher, 2000; Wu et al., 1999).

We tested the idea that a second Ca^{2+} binding site is responsible for the induction of facilitation by modelling the Ca^{2+} dependence of facilitation. Therefore, we recorded frequency facilitation at different extracellular Ca^{2+} concentrations.
The most straight forward explanation of how frequency facilitation arises is that a

[1]Enzymkinetik. Theorie und Methoden, Vol.3, 2000 by Hans Bisswanger

second Ca^{2+} binding site modifies release during repetitive stimulations. Therefore, we developed a mathematical model incorporating two Ca^{2+} binding sites. Our model assumed that both sensors can interact, and that Ca^{2+} binding to the second, the frequency facilitation sensor, increases the Ca^{2+} affinity of the first, the release sensor. It has been proposed that an increase in Ca^{2+} affinity can be a consequence of an enhanced Ca^{2+} sensitivity of the Ca^{2+} binding site or likewise, a closer coupling of the senor to the Ca^{2+} entry site (for review: Zucker and Regehr, 2002).
The interstimulus interval (ISI), the stimulation number (i), the cooperativity level of baseline transmission (n), and the intracellular Ca^{2+} concentration (Ca_{int}) were given parameters. In contrast, the relative affinity of the release sensor (Kd_{rel}) and the frequency facilitation sensor (Kd_{FF}), the Ca^{2+} unbinding rate (K_{off}), the level of cooperativity of the frequency facilitation sensor (m), and the release fraction (rf) have been determined by the fitting procedure. The proportionality constant *coup* stands for an unknown process, that links the frequency facilitation sensor to the release sensor. Also *coup* has been determined by the fitting procedure.

When we fitted our recorded data with a model where non-cooperative binding of Ca^{2+} ions at the frequency facilitation sensor occurs this resulted in unphysiological values for the model parameters. Therefore, we next tried a model with cooperative binding. With this model we could fit simultaneously multiple data sets (1 Hz and 0.3 Hz). From this it became obvious, that our model describes frequency facilitation in most situations rather accurately, but shows some limitations at early stimulations.
We made some assumptions to limit the complexity of the model. Therefore, the model does not incorporate other mechanisms that might contribute to frequency facilitation in addition to the change in Ca^{2+} affinity of the release sensor. These alternative mechanisms could be: Recruitment of new release sites, spike broadening, enhanced Ca^{2+} influx, or afterpotentials (for review: Zucker and Regehr, 2002). At low Ca^{2+} concentrations MF-fEPSPs were smallest and have therefore been influenced most by background noise in the recorded signal. Therefore, we excluded

these data points from further analysis. To increase the Ca^{2+} concentration beyond 5 mM, we had to use HEPES buffered ACSF instead of carbogene buffered. Furthermore, at these concentrations we were not able to keep the divalent cation concentration constant by decreasing the Mg^{2+} concentration. This could alter the surface charge at the plasma membrane and could lead to artificial changes of the MF-fEPSP amplitudes.

Nevertheless, there are some interesting results of the modelling.

As proposed (Blundon et al., 1993; Winslow et al., 1994), our model predicts a high Ca^{2+} affinity for the frequency facilitation sensor relative to the release sensor ($Kd_{FF} = 0.05$, $Kd_{rel} = 2.64$). To determine the Ca^{2+} unbinding kinetics, we can calculate the time constant (τ) of the unbinding from the unbinding rate K_{off}:

$$\tau = \frac{1}{K_{off}} \tag{5.1}$$

Therefore, our model predicts that Ca^{2+} unbinds from the frequency facilitation sensor with $\tau = 7$ s. This fits to the observation that frequency facilitation can be induced even at rather low stimulation frequencies (e.g. 0.3 Hz). Finally, the level of cooperativity ($m \approx 4$) is in the same range as suggested for other Ca^{2+} sensors (Bollmann et al., 2000; Sakaba and Neher, 2001; Schneggenburger and Neher, 2000; Wu et al., 1999) and is similar to the value obtained for baseline transmission at the MF-CA3 synapse.

It has been reported that at MF-CA3 synapses the refilling of the RRP from the reserve-pool has a time constant of $\tau \approx$15 s (Suyama et al., 2007). We investigated if refilling contributes to saturation of facilitation. Therefore, we measured facilitation at different Ca^{2+} concentrations. These experiments revealed that saturation of facilitation is independent of the refilling of the RRP at stimulation intervals $>$ 40 ms. These experiments does not rule out the possibility, that vesicle refilling itself is Ca^{2+} dependent.

In the past several years efforts have been made to identify the Ca^{2+} sensor molecules responsible for transmitter release. Several observations revealed members of the

synaptotagmin family as the main Ca^{2+} sensor molecules mediating basal transmitter release (Geppert et al., 1994; Tang et al., 2006).

There are 15 synaptotagmin isoforms expressed in vertebrates (Mittelstaedt et al., 2009; Ullrich and Südhof, 1995). These isoforms are differentially expressed in the brain, exhibit different Ca^{2+} affinities, and have been shown to differentially influence release (Bhalla et al., 2005; Maximov et al., 2007; Pang et al., 2006; Saraswati et al., 2007; Sun et al., 2007). From the 15 isoforms, synaptotagmin-1, -2, and -9 are known to play an essential role in baseline synaptic transmission (Xu et al., 2007). Furthermore, Gustavsson et al. (2009) showed a role of synaptotagmin-7 in glucagon release from endocrine cells in the pancreas. The function of the remaining synaptotagmin isoforms is so far unclear.

The C2A and C2B Ca^{2+} binding domains are only conserved in synaptotagmins 1 - 7 and 9 - 10 (Bhalla et al., 2005; Rickman et al., 2004). The C2A-domain binds up to three Ca^{2+} ions, the C2B-domain up to two. This would fit to the estimated level of cooperativity, requiring the binding of four Ca^{2+} ions at the frequency facilitation sensor.

Among the synaptotagmin isoforms, synaptotagmin-6 and -10 are expressed in dentate gyrus granule cells and not, or only weakly, in other parts of the hippocampus (Mittelstaedt et al., 2009). The C2A-domain of synaptotagmin-10 has been shown to have an EC_{50} of about 10 - 20 μM Ca^{2+} (Sugita et al., 2002). In contrast, it has been estimated that synaptotagmin-1 has an EC_{50} ten times lower (about 3 μM) (Li et al., 1995; Sugita et al., 2002). The EC_{50} value for synaptotagmin-6 is not available, but synaptotagmin-6 and -10 are highly homologue. Therefore similar EC_{50} values can be expected.

αCamKII has been shown to influence several forms of synaptic plasticity (Elgersma et al., 2002; Salin et al., 1996; Zhang et al., 2005) and αCamKII is known to phosphorylate synapsins in a Ca^{2+} dependent manner. It was shown by Salin et al. (1996) that application of the selective CamKII inhibitor KN-62 reduces the amount of frequency facilitation at MF-CA3 synapses.

In our hands, application of the same inhibitor and of another inhibitor (KN-93) did not alter frequency facilitation. We also investigated frequency facilitation in αCamKII null-mutants (Elgersma et al., 2002), but knockout animals and littermate controls showed similar levels of frequency facilitation. Taken together, we could show that there is no influence of αCamKII on MF-CA3 frequency facilitation.

In contrast to other synapses of the hippocampus, LTP at the MF-CA3 synapse is induced and expressed presynaptically. It has been reported that mossy fiber LTP is induced by Ca^{2+} dependent activation of adenylate cyclase (Weisskopf et al., 1994) (for review: Nicoll and Schmitz, 2005). This leads to the activation of PKA, which causes a persistent increase in synaptic strength. Interestingly, it has been shown that there is a PKA dependent phosphorylation of synapsins (Hilfiker et al., 1999). In our recordings, inhibition of PKA did not influence frequency facilitation.

Moreover, MAPK has been reported to be involved in the induction of postsynaptic LTP (Waltereit and Weller, 2003). MAPK is known to phosphorylate synapsins in a Ca^{2+} dependent manner (Hilfiker et al., 1999). Therefore, we tested for a role of MAPK in frequency facilitation, but found facilitation unchanged following MAPK inhibition.

Moreover, in chromaffin cells an enhanced recovery from depression after elevation of extracellular Ca^{2+} has been observed (Dinkelacker et al., 2000; Smith et al., 1998). This enhancement is mediated by PKC dependent and independent processes. A PKC dependent increase of the RRP size in hippocampal cell cultures has already been reported by Stevens and Sullivan (1998). It was shown that post-tetanic potentiation (PTP) at the Calyx of Held relies predominately on the Ca^{2+} dependent activation of presynaptic PKC (Korogod et al., 2007). Although PTP at the Calyx of Held is accompanied by an increase of the presynaptic Ca^{2+} transients, the potentiation of transmitter release is mainly caused by an PKC mediated enhancement of the Ca^{2+} sensitivity of vesicle fusion. Because a similar PKC mediated mechanism could also be responsible for frequency facilitation, we tested the role of PKC in frequency facilitation at MF-CA3 synapses. We found no change in frequency

facilitation by application of a PKC blocker.

Recently, it was reported that frequency facilitation at MF-CA3 synapses depends in part on the interaction of synapsin with f-actin (Owe et al., 2009). We tested for a role of f-actin in frequency facilitation by application of f-actin stabilizing and destabilizing agents, but found no change in frequency facilitation.
In contrast, Owe et al. (2009) found a reduction of frequency facilitation by application of the f-actin destabilizing agent cytochalasin B. Although we used latrunkulin A instead of cytochalasin B, there is an obvious difference in our results compared to Owe et al. (2009).
Owe et al. (2009) used a bath Ca^{2+} concentration of 1 mM (2.5 mM in our recordings). We have shown that STP at the MF-CA3 synapse is strongly influenced by the extracellular Ca^{2+} concentration and we cannot exclude that frequency facilitation is differentially induced at different Ca^{2+} concentrations.
But there is another obvious difference in the recording conditions of Owe et al. (2009). The authors incubated the slices for 120 min with cytochalasin B. In contrast, we incubated the slices for only 60 min with latrunkulin A. Interestingly, Owe et al. (2009) found a baseline reduction after application of cytochalasin B. In contrast, there was no obvious change in baseline transmission in our recordings. The baseline reduction reported by Owe et al. (2009) could either be a consequence of the reorganization of presynaptic vesicles inside mossy fiber terminals or an implication of neuronal cell death at dentate gyrus granule cells caused by application of cytochalasin B. Cytochalasin B induced apoptosis of dentate gyrus granule cells has already been reported (Kim et al., 2002), although on a larger time scale.
Although we already tested for a role of different kinases in MF-CA3 frequency facilitation, we also tested for a role of phosphatases. It was shown that protein phosphatases can influence transmitter release. Although they play predominantly a role in the induction of long-term depression (LTD) (for review: Manabe, 1997) or depotentiation of LTP (Huang et al., 2002), we tested for a role in frequency facilitation. Combined blockade of the phosphatases 1, 2A, and calcineurin did not

affect frequency facilitation.

Several studies suggested a role of presynaptic KA autoreceptors in MF-CA3 frequency facilitation (Breustedt and Schmitz, 2004; Contractor et al., 2001; Kamiya et al., 2002; Schmitz et al., 2001). Furthermore, it has been proposed that the additional Ca^{2+} influx through KARs causes Ca^{2+} release from intracellular stores (Lauri et al., 2003), contributing to the potentiation of release. However, MF-CA3 frequency facilitation can be recorded in the presence of KAR blockers (Salin et al., 1996). Furthermore, Kwon and Castillo (2008) showed that KARs do not facilitate transmitter release over a wide range of stimulation frequencies. In addition we recorded MF-CA3 frequency facilitation after application of the specific KAR inhibitor NS-102 (10 μM). We could observe no change in frequency facilitation. In summary, an involvement of presynaptic KARs in MF-CA3 frequency facilitation is most unlikely.

In conclusion, our results suggest that MF-CA3 frequency facilitation is a robust phenomenon that occurs during low frequency stimulation of mossy fiber axons. It relies preferentially on the influx of Ca^{2+} ions into the presynaptic terminal, but is independent of the Ca^{2+} influx pathway and of an accumulation of presynaptic bulk Ca^{2+}. It is most likely induced by a second Ca^{2+} binding site apart from the one responsible for baseline synaptic transmission. Moreover, we can exclude a contribution of a large number of presynaptic kinases and phosphatases or a dependence on the integrity of the cytoskeleton.
These data are consistent with a more direct Ca^{2+}-dependent mechanism acting directly on the release machinery.

Bibliography

Abe, T., Sugihara, H., Nawa, H., Shigemoto, R., Mizuno, N., and Nakanishi, S. (1992). Molecular characterization of a novel metabotropic glutamate receptor mglur5 coupled to inositol phosphate/calcium signal transduction. *J Biol Chem*, 267(19):13361–13368.

Acsády, L., Kamondi, A., Sík, A., Freund, T., and Buzsáki, G. (1998). GABA-ergic cells are the major postsynaptic targets of mossy fibers in the rat hippocampus. *J Neurosci*, 18(9):3386–3403.

Adler, E. M., Augustine, G. J., Duffy, S. N., and Charlton, M. P. (1991). Alien intracellular calcium chelators attenuate neurotransmitter release at the squid giant synapse. *J Neurosci*, 11(6):1496–1507.

Amaral, D. G. and Dent, J. A. (1981). Development of the mossy fibers of the dentate gyrus: I. a light and electron microscopic study of the mossy fibers and their expansions. *J Comp Neurol*, 195(1):51–86.

Amaral, D. G., Ishizuka, N., and Claiborne, B. (1990). Neurons, numbers and the hippocampal network. *Prog Brain Res*, 83:1–11.

Amaral, D. G. and Witter, M. P. (1989). The three-dimensional organization of the hippocampal formation: a review of anatomical data. *Neuroscience*, 31(3):571–591.

Barker, L. A., Dowdall, M. J., and Whittaker, V. P. (1972). Choline metabolism

in the cerebral cortex of guinea pigs. stable-bound acetylcholine. *Biochem J*, 130(4):1063–1075.

Bear, M. F. and Malenka, R. C. (1994). Synaptic plasticity: LTP and LTD. *Curr Opin Neurobiol*, 4(3):389–399.

Bennett, M. R. (1999). The concept of a calcium sensor in transmitter release. *Prog Neurobiol*, 59(3):243–277.

Bhalla, A., Tucker, W. C., and Chapman, E. R. (2005). Synaptotagmin isoforms couple distinct ranges of calcium, barium, and strontium concentration to snare-mediated membrane fusion. *Mol Biol Cell*, 16(10):4755–4764.

Blackstad, T. W., Brink, K., Hem, J., and Jeune, B. (1970). Distribution of hippocampal mossy fibers in the rat. an experimental study with silver impregnation methods. *J Comp Neurol*, 138(4):433–449.

Blatow, M., Caputi, A., Burnashev, N., Monyer, H., and Rozov, A. (2003). Calcium buffer saturation underlies paired pulse facilitation in calbindin-d28k-containing terminals. *Neuron*, 38(1):79–88.

Blundon, J. A., Wright, S. N., Brodwick, M. S., and Bittner, G. D. (1993). Residual free calcium is not responsible for facilitation of neurotransmitter release. *Proc Natl Acad Sci U S A*, 90(20):9388–9392.

Bollmann, J. H., Sakmann, B., and Borst, J. G. (2000). Calcium sensitivity of glutamate release in a calyx-type terminal. *Science*, 289(5481):953–957.

Bolshakov, V. Y. and Siegelbaum, S. A. (1995). Regulation of hippocampal transmitter release during development and long-term potentiation. *Science*, 269(5231):1730–1734.

Breustedt, J. and Schmitz, D. (2004). Assessing the role of GLUK5 and GLUK6 at hippocampal mossy fiber synapses. *J Neurosci*, 24(45):10093–10098.

Brown, T. H. and Johnston, D. (1983). Voltage-clamp analysis of mossy fiber synaptic input to hippocampal neurons. *J Neurophysiol*, 50(2):487–507.

Castillo, P. E., Salin, P. A., Weisskopf, M. G., and Nicoll, R. A. (1996). Characterizing the site and mode of action of dynorphin at hippocampal mossy fiber synapses in the guinea pig. *J Neurosci*, 16(19):5942–5950.

Castillo, P. E., Weisskopf, M. G., and Nicoll, R. A. (1994). The role of calcium channels in hippocampal mossy fiber synaptic transmission and long-term potentiation. *Neuron*, 12(2):261–269.

Cavazzini, M., Bliss, T., and Emptage, N. (2005). Calcium and synaptic plasticity. *Cell Calcium*, 38(3-4):355–367.

Ceccarelli, B., Hurlbut, W. P., and Mauro, A. (1973). Turnover of transmitter and synaptic vesicles at the frog neuromuscular junction. *J Cell Biol*, 57(2):499–524.

Claiborne, B. J., Amaral, D. G., and Cowan, W. M. (1986). A light and electron microscopic analysis of the mossy fibers of the rat dentate gyrus. *J Comp Neurol*, 246(4):435–458.

Contractor, A., Swanson, G., and Heinemann, S. F. (2001). Kainate receptors are involved in short- and long-term plasticity at mossy fiber synapses in the hippocampus. *Neuron*, 29(1):209–216.

Cummings, D. D., Wilcox, K. S., and Dichter, M. A. (1996). Calcium-dependent paired-pulse facilitation of miniature EPSC frequency accompanies depression of EPSCs at hippocampal synapses in culture. *J Neurosci*, 16(17):5312–5323.

Darstein, M., Petralia, R. S., Swanson, G. T., Wenthold, R. J., and Heinemann, S. F. (2003). Distribution of kainate receptor subunits at hippocampal mossy fiber synapses. *J Neurosci*, 23(22):8013–8019.

Delaney, K. R., Zucker, R. S., and Tank, D. W. (1989). Calcium in motor nerve terminals associated with posttetanic potentiation. *J Neurosci*, 9(10):3558–3567.

Deller, T., Nitsch, R., and Frotscher, M. (1994). Associational and commissural afferents of parvalbumin-immunoreactive neurons in the rat hippocampus: a combined immunocytochemical and PHA-L study. *J Comp Neurol*, 350(4):612–622.

Dietrich, D., Kirschstein, T., Kukley, M., Pereverzev, A., von der Brelie, C., Schneider, T., and Beck, H. (2003). Functional specialization of presynaptic Cav2.3 calcium channels. *Neuron*, 39(3):483–496.

Dinkelacker, V., Voets, T., Neher, E., and Moser, T. (2000). The readily releasable pool of vesicles in chromaffin cells is replenished in a temperature-dependent manner and transiently overfills at 37 degrees c. *J Neurosci*, 20(22):8377–8383.

Dobrunz, L. E. and Stevens, C. F. (1997). Heterogeneity of release probability, facilitation, and depletion at central synapses. *Neuron*, 18(6):995–1008.

Dodge, F. A. and Rahamimoff, R. (1967). On the relationship between calcium concentration and the amplitude of the end-plate potential. *J Physiol*, 189(2):90P–92P.

Dulubova, I., Sugita, S., Hill, S., Hosaka, M., Fernandez, I., Südhof, T. C., and Rizo, J. (1999). A conformational switch in syntaxin during exocytosis: role of munc18. *EMBO J*, 18(16):4372–4382.

Elgersma, Y., Fedorov, N. B., Ikonen, S., Choi, E. S., Elgersma, M., Carvalho, O. M., Giese, K. P., and Silva, A. J. (2002). Inhibitory autophosphorylation of CamKII controls PSD association, plasticity, and learning. *Neuron*, 36(3):493–505.

Fisher, S. A., Fischer, T. M., and Carew, T. J. (1997). Multiple overlapping processes underlying short-term synaptic enhancement. *Trends Neurosci*, 20(4):170–177.

Geppert, M., Goda, Y., Hammer, R. E., Li, C., Rosahl, T. W., Stevens, C. F., and Südhof, T. C. (1994). Synaptotagmin I: a major calcium sensor for transmitter release at a central synapse. *Cell*, 79(4):717–727.

Goda, Y. and Stevens, C. F. (1994). Two components of transmitter release at a central synapse. *Proc Natl Acad Sci USA*, 91(26):12942–12946.

Gottlieb, D. I. and Cowan, W. M. (1973). Autoradiographic studies of the commissural and ipsilateral association connection of the hippocampus and detentate gyrus of the rat. I. The commissural connections. *J Comp Neurol*, 149(4):393–422.

Gundlfinger, A., Bischofberger, J., Johenning, F. W., Torvinen, M., Schmitz, D., and Breustedt, J. (2007). Adenosine modulates transmission at the hippocampal mossy fibre synapse via direct inhibition of presynaptic calcium channels. *J Physiol*, 582(Pt 1):263–277.

Gustavsson, N., Wei, S.-H., Hoang, D. N., Lao, Y., Zhang, Q., Radda, G. K., Rorsman, P., Sudhof, T. C., and Han, W. (2009). Synaptotagmin-7 is a principal calcium-sensor for calcium-induced glucagon exocytosis in pancreas. *J Physiol*.

Helmchen, F., Borst, J. G., and Sakmann, B. (1997). Calcium dynamics associated with a single action potential in a cns presynaptic terminal. *Biophys J*, 72(3):1458–1471.

Heuser, J. E. and Reese, T. S. (1973). Evidence for recycling of synaptic vesicle membrane during transmitter release at the frog neuromuscular junction. *J Cell Biol*, 57(2):315–344.

Hilfiker, S., Pieribone, V. A., Czernik, A. J., Kao, H. T., Augustine, G. J., and Greengard, P. (1999). Synapsins as regulators of neurotransmitter release. *Philos Trans R Soc Lond B Biol Sci*, 354(1381):269–279.

Hojjati, M. R., van Woerden, G. M., Tyler, W. J., Giese, K. P., Silva, A. J., Pozzo-Miller, L., and Elgersma, Y. (2007). Kinase activity is not required for alphaCamKII-dependent presynaptic plasticity at CA3-CA1 synapses. *Nat Neurosci*, 10(9):1125–1127.

Huang, C.-C., Chen, Y.-L., Liang, Y.-C., and Hsu, K.-S. (2002). Role for cAMP and protein phosphatase in the presynaptic expression of mouse hippocampal mossy fibre depotentiation. *J Physiol*, 543(Pt 3):767–778.

Iino, M. (2006). Calcium-dependent inositol 1,4,5-trisphosphate and nitric oxide signaling in cerebellar neurons. *J Pharmacol Sci*, 100(5):538–544.

Jahn, R., Lang, T., and Südhof, T. C. (2003). Membrane fusion. *Cell*, 112(4):519–533.

Kamiya, H., Ozawa, S., and Manabe, T. (2002). Kainate receptor-dependent short-term plasticity of presynaptic calcium influx at the hippocampal mossy fiber synapses. *J Neurosci*, 22(21):9237–9243.

Kamiya, H., Shinozaki, H., and Yamamoto, C. (1996). Activation of metabotropic glutamate receptor type 2/3 suppresses transmission at rat hippocampal mossy fibre synapses. *J Physiol*, 493 (Pt 2):447–455.

Kamiya, H. and Zucker, R. S. (1994). Residual calcium and short-term synaptic plasticity. *Nature*, 371(6498):603–606.

Katz, B. and Miledi, R. (1967). The timing of calcium action during neuromuscular transmission. *J Physiol*, 189(3):535–544.

Katz, B. and Miledi, R. (1968). The role of calcium in neuromuscular facilitation. *J Physiol*, 195(2):481–492.

Kim, J.-A., Mitsukawa, K., Yamada, M. K., Nishiyama, N., Matsuki, N., and Ikegaya, Y. (2002). Cytoskeleton disruption causes apoptotic degeneration of dentate granule cells in hippocampal slice cultures. *Neuropharmacology*, 42(8):1109–1118.

Korogod, N., Lou, X., and Schneggenburger, R. (2007). Posttetanic potentiation critically depends on an enhanced calcium sensitivity of vesicle fusion mediated by presynaptic PKC. *Proc Natl Acad Sci U S A*, 104(40):15923–15928.

Kukley, M., Schwan, M., Fredholm, B. B., and Dietrich, D. (2005). The role of extracellular adenosine in regulating mossy fiber synaptic plasticity. *J Neurosci*, 25(11):2832–2837.

Kwon, H.-B. and Castillo, P. E. (2008). Role of glutamate autoreceptors at hippocampal mossy fiber synapses. *Neuron*, 60(6):1082–1094.

Lauri, S. E., Bortolotto, Z. A., Nistico, R., Bleakman, D., Ornstein, P. L., Lodge, D., Isaac, J. T. R., and Collingridge, G. L. (2003). A role for calcium stores in kainate receptor-dependent synaptic facilitation and LTP at mossy fiber synapses in the hippocampus. *Neuron*, 39(2):327–341.

Lei, S. and McBain, C. J. (2002). Distinct NMDA receptors provide differential modes of transmission at mossy fiber-interneuron synapses. *Neuron*, 33(6):921–933.

Leibold, C., Gundlfinger, A., Schmidt, R., Thurley, K., Schmitz, D., and Kempter, R. (2008). Temporal compression mediated by short-term synaptic plasticity. *Proc Natl Acad Sci U S A*, 105(11):4417–4422.

Li, C., Ullrich, B., Zhang, J. Z., Anderson, R. G., Brose, N., and Südhof, T. C. (1995). Calcium-dependent and -independent activities of neural and non-neural synaptotagmins. *Nature*, 375(6532):594–599.

Li, X. G., Somogyi, P., Ylinen, A., and Buzsáki, G. (1994). The hippocampal CA3 network: an in vivo intracellular labeling study. *J Comp Neurol*, 339(2):181–208.

Llinás, R. R., Sugimori, M., and Silver, R. B. (1994). Localization of calcium concentration microdomains at the active zone in the squid giant synapse. *Adv Second Messenger Phosphoprotein Res*, 29:133–137.

Loewi, O. (1921). Über humorale Übertragbarkeit der herznervenwirkung. *Pflügers Arch. ges. Physiol.*, 193:239–242.

Manabe, T. (1997). Two forms of hippocampal long-term depression, the counterpart of long-term potentiation. *Rev Neurosci*, 8(3-4):179–193.

Maximov, A., Shin, O.-H., Liu, X., and Südhof, T. C. (2007). Synaptotagmin-12, a synaptic vesicle phosphoprotein that modulates spontaneous neurotransmitter release. *J Cell Biol*, 176(1):113–124.

Meinrenken, C. J., Borst, J. G. G., and Sakmann, B. (2003). Local routes revisited: The space and time dependence of the calcium signal for phasic transmitter release at the rat calyx of held. *J Physiol*, 547(Pt 3):665–689.

Miledi, R. (1973). Transmitter release induced by injection of calcium ions into nerve terminals. *Proc R Soc Lond B Biol Sci*, 183(73):421–425.

Mittelstaedt, T., Seifert, G., Alvárez-Barón, E., Steinhäuser, C., Becker, A. J., and Schoch, S. (2009). Differential mRNA expression patterns of the synaptotagmin gene family in the rodent brain. *J Comp Neurol*, 512(4):514–528.

Moore, K. A., Nicoll, R. A., and Schmitz, D. (2003). Adenosine gates synaptic plasticity at hippocampal mossy fiber synapses. *Proc Natl Acad Sci USA*, 100(24):14397–14402.

Moser, E., Moser, M. B., and Andersen, P. (1993). Synaptic potentiation in the rat dentate gyrus during exploratory learning. *Neuroreport*, 5(3):317–320.

Neher, E. and Sakaba, T. (2001). Estimating transmitter release rates from postsynaptic current fluctuations. *J Neurosci*, 21(24):9638–9654.

Nicoll, R. A. and Schmitz, D. (2005). Synaptic plasticity at hippocampal mossy fibre synapses. *Nat Rev Neurosci*, 6(11):863–876.

Owe, S. G., Jensen, V., Evergren, E., Ruiz, A., Shupliakov, O., Kullmann, D. M., Storm-Mathisen, J., Walaas, S. I., Øivind Hvalby, and Bergersen, L. H. (2009). Synapsin- and actin-dependent frequency enhancement in mouse hippocampal mossy fiber synapses. *Cereb Cortex*, 19(3):511–523.

Pang, Z. P., Shin, O.-H., Meyer, A. C., Rosenmund, C., and Südhof, T. C. (2006). A gain-of-function mutation in synaptotagmin-1 reveals a critical role of calcium-dependent soluble N-ethylmaleimide-sensitive factor attachment protein receptor complex binding in synaptic exocytosis. *J Neurosci*, 26(48):12556–12565.

Pongs, O., Lindemeier, J., Zhu, X. R., Theil, T., Engelkamp, D., Krah-Jentgens, I., Lambrecht, H. G., Koch, K. W., Schwemer, J., and Rivosecchi, R. (1993). Frequenin–a novel calcium-binding protein that modulates synaptic efficacy in the drosophila nervous system. *Neuron*, 11(1):15–28.

Rahamimoff, R. and Dodge, F. A. (1969). Regulation of transmitter release at the neuromuscular synapse: The cooperative hypothesis. *Electroencephalogr Clin Neurophysiol*, 27(2):219.

Reid, C. A., Bekkers, J. M., and Clements, J. D. (2003). Presynaptic ca2+ channels: a functional patchwork. *Trends Neurosci*, 26(12):683–687.

Reim, K., Mansour, M., Varoqueaux, F., McMahon, H. T., Südhof, T. C., Brose, N., and Rosenmund, C. (2001). Complexins regulate a late step in calcium-dependent neurotransmitter release. *Cell*, 104(1):71–81.

Rickman, C., Craxton, M., Osborne, S., and Davletov, B. (2004). Comparative analysis of tandem C2 domains from the mammalian synaptotagmin family. *Biochem J*, 378(Pt 2):681–686.

Rosahl, T. W., Geppert, M., Spillane, D., Herz, J., Hammer, R. E., Malenka, R. C., and Südhof, T. C. (1993). Short-term synaptic plasticity is altered in mice lacking synapsin I. *Cell*, 75(4):661–670.

Rosahl, T. W., Spillane, D., Missler, M., Herz, J., Selig, D. K., Wolff, J. R., Hammer, R. E., Malenka, R. C., and Südhof, T. C. (1995). Essential functions of synapsins I and II in synaptic vesicle regulation. *Nature*, 375(6531):488–493.

Rozov, A., Burnashev, N., Sakmann, B., and Neher, E. (2001). Transmitter release modulation by intracellular calcium buffers in facilitating and depressing nerve

terminals of pyramidal cells in layer 2/3 of the rat neocortex indicates a target cell-specific difference in presynaptic calcium dynamics. *J Physiol*, 531(Pt 3):807–826.

Ryan, T. A., Li, L., Chin, L. S., Greengard, P., and Smith, S. J. (1996). Synaptic vesicle recycling in synapsin I knock-out mice. *J Cell Biol*, 134(5):1219–1227.

Sakaba, T. and Neher, E. (2001). Quantitative relationship between transmitter release and calcium current at the calyx of held synapse. *J Neurosci*, 21(2):462–476.

Sakaba, T., Schneggenburger, R., and Neher, E. (2002). Estimation of quantal parameters at the calyx of held synapse. *Neurosci Res*, 44(4):343–356.

Salin, P. A., Scanziani, M., Malenka, R. C., and Nicoll, R. A. (1996). Distinct short-term plasticity at two excitatory synapses in the hippocampus. *Proc Natl Acad Sci USA*, 93(23):13304–13309.

Saraswati, S., Adolfsen, B., and Littleton, J. T. (2007). Characterization of the role of the synaptotagmin family as calcium sensors in facilitation and asynchronous neurotransmitter release. *Proc Natl Acad Sci U S A*, 104(35):14122–14127.

Schmitz, D., Mellor, J., and Nicoll, R. A. (2001). Presynaptic kainate receptor mediation of frequency facilitation at hippocampal mossy fiber synapses. *Science*, 291(5510):1972–1976.

Schneggenburger, R., Meyer, A. C., and Neher, E. (1999). Released fraction and total size of a pool of immediately available transmitter quanta at a calyx synapse. *Neuron*, 23(2):399–409.

Schneggenburger, R. and Neher, E. (2000). Intracellular calcium dependence of transmitter release rates at a fast central synapse. *Nature*, 406(6798):889–893.

Scoville, W. B. and Milner, B. (1957). Loss of recent memory after bilateral hippocampal lesions. *J Neurol Neurosurg Psychiatry*, 20(1):11–21.

Südhof, T. C. (2004). The synaptic vesicle cycle. *Annu Rev Neurosci*, 27:509–547.

Shain, W. and Carpenter, D. O. (1981). Mechanisms of synaptic modulation. *Int Rev Neurobiol*, 22:205–250.

Shimizu, H., Fukaya, M., Yamasaki, M., Watanabe, M., Manabe, T., and Kamiya, H. (2008). Use-dependent amplification of presynaptic calcium signaling by axonal ryanodine receptors at the hippocampal mossy fiber synapse. *Proc Natl Acad Sci U S A*, 105(33):11998–12003.

Sik, A., Tamamaki, N., and Freund, T. F. (1993). Complete axon arborization of a single CA3 pyramidal cell in the rat hippocampus, and its relationship with postsynaptic parvalbumin-containing interneurons. *Eur J Neurosci*, 5(12):1719–1728.

Silva, A. J., Stevens, C. F., Tonegawa, S., and Wang, Y. (1992). Deficient hippocampal long-term potentiation in alpha-calcium-calmodulin kinase II mutant mice. *Science*, 257(5067):201–206.

Sippy, T., Cruz-Martín, A., Jeromin, A., and Schweizer, F. E. (2003). Acute changes in short-term plasticity at synapses with elevated levels of neuronal calcium sensor-1. *Nat Neurosci*, 6(10):1031–1038.

Smith, C., Moser, T., Xu, T., and Neher, E. (1998). Cytosolic calcium acts by two separate pathways to modulate the supply of release-competent vesicles in chromaffin cells. *Neuron*, 20(6):1243–1253.

Squire, L. R. and Zola-Morgan, S. (1991). The medial temporal lobe memory system. *Science*, 253(5026):1380–1386. review.

Stanton, P. K. and Gage, A. T. (1996). Distinct synaptic loci of calcium/calmodulin-dependent protein kinase II necessary for long-term potentiation and depression. *J Neurophysiol*, 76(3):2097–2101.

Stevens, C. F. and Sullivan, J. M. (1998). Regulation of the readily releasable vesicle pool by protein kinase c. *Neuron*, 21(4):885–893.

Sugita, S., Shin, O.-H., Han, W., Lao, Y., and Südhof, T. C. (2002). Synaptotagmins form a hierarchy of exocytotic calcium sensors with distinct calcium affinities. *EMBO J*, 21(3):270–280.

Sun, J., Pang, Z. P., Qin, D., Fahim, A. T., Adachi, R., and Südhof, T. C. (2007). A dual-calcium-sensor model for neurotransmitter release in a central synapse. *Nature*, 450(7170):676–682.

Suyama, S., Hikima, T., Sakagami, H., Ishizuka, T., and Yawo, H. (2007). Synaptic vesicle dynamics in the mossy fiber-CA3 presynaptic terminals of mouse hippocampus. *Neurosci Res*, 59(4):481–490.

Swandulla, D., Hans, M., Zipser, K., and Augustine, G. J. (1991). Role of residual calcium in synaptic depression and posttetanic potentiation: Fast and slow calcium signaling in nerve terminals. *Neuron*, 7(6):915–926.

T. W. Blackstad, T. W. and Kjaerheim, A. (1961). Special axo-dendritic synapses in the hippocampal cortex: electron and light microscopic studies on the layer of mossy fibers. *J Comp Neurol*, 117:133–159.

Tang, J., Maximov, A., Shin, O.-H., Dai, H., Rizo, J., and Südhof, T. C. (2006). A complexin/synaptotagmin 1 switch controls fast synaptic vesicle exocytosis. *Cell*, 126(6):1175–1187.

Ullrich, B. and Südhof, T. C. (1995). Differential distributions of novel synaptotagmins: comparison to synapsins. *Neuropharmacology*, 34(11):1371–1377.

Urban, N. N., Henze, D. A., and Barrionuevo, G. (2001). Revisiting the role of the hippocampal mossy fiber synapse. *Hippocampus*, 11(4):408–417.

Waltereit, R. and Weller, M. (2003). Signaling from cAMP/PKA to MAPK and synaptic plasticity. *Mol Neurobiol*, 27(1):99–106.

Weisskopf, M. G., Castillo, P. E., Zalutsky, R. A., and Nicoll, R. A. (1994). Mediation of hippocampal mossy fiber long-term potentiation by cyclic AMP. *Science*, 265(5180):1878–1882.

Winslow, J. L., Duffy, S. N., and Charlton, M. P. (1994). Homosynaptic facilitation of transmitter release in crayfish is not affected by mobile calcium chelators: Implications for the residual ionized calcium hypothesis from electrophysiological and computational analyses. *J Neurophysiol*, 72(4):1769–1793.

Wu, L. G., Westenbroek, R. E., Borst, J. G., Catterall, W. A., and Sakmann, B. (1999). Calcium channel types with distinct presynaptic localization couple differentially to transmitter release in single calyx-type synapses. *J Neurosci*, 19(2):726–736.

Xu, J., Mashimo, T., and Südhof, T. C. (2007). Synaptotagmin-1, -2, and -9: Calcium sensors for fast release that specify distinct presynaptic properties in subsets of neurons. *Neuron*, 54(4):567–581.

Zhang, L., Kirschstein, T., Sommersberg, B., Merkens, M., Manahan-Vaughan, D., Elgersma, Y., and Beck, H. (2005). Hippocampal synaptic metaplasticity requires inhibitory autophosphorylation of calcium/calmodulin-dependent kinase II. *J Neurosci*, 25(33):7697–7707.

Zucker, R. S. and Regehr, W. G. (2002). Short-term synaptic plasticity. *Annu Rev Physiol*, 64:355–405.

Zucker, R. S. and Stockbridge, N. (1983). Presynaptic calcium diffusion and the time courses of transmitter release and synaptic facilitation at the squid giant synapse. *J Neurosci*, 3(6):1263–1269.

Appendix A

Estimation of release probability

The release probability (p) represents the probability of a vesicle to fuse with the presynaptic membrane. Therefore $p = 1$ would indicate the situation in which all available vesicles would fuse upon stimulation. In this situation transmitter release is saturated and cannot further increased without recruiting new release sites.
The plot of the relative fEPSP amplitudes (Fig.A.1, 15^{th} peak at 1 or 0.3 Hz divided by the mean of baseline at 1.16 mM Ca_{int}) shows a sigmoidal course that saturates at high Ca^{2+} concentrations. Assuming that no new release sites are recruited during frequency facilitation, we fitted the data with a Hill equation (Fig.A.1). Unfortunately, we could not rise Ca_{ext} more than 10 mM corresponding to 2.03 mM Ca_{int}. Therefore the value of the level of the plateau has to be considered as an estimate. This estimation allows us to calculate the release probability (Sakaba et al., 2002) at baseline conditions:

$$p = 100 \div R_{max} \tag{A.1}$$

The coefficient R_{max} stands for the maximal transmitter release (in %). We calculated a release probability of $p \approx 0.06$ at 1.16 mM Ca_{int}. This is rather low compared to other cortical synapses; e.g. release probability at the Schaffer collateral pathway

has been estimated to be about 0.5 - 0.9 (Bolshakov and Siegelbaum, 1995; Dobrunz and Stevens, 1997).

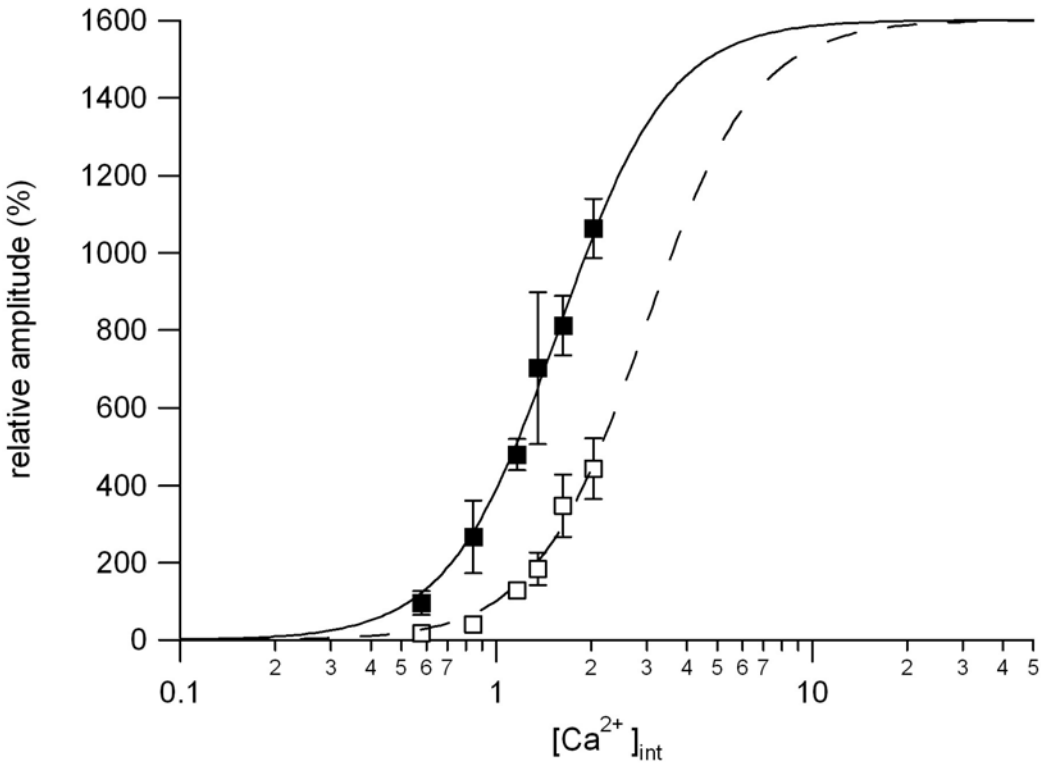

Figure A.1: ***Estimation of the release probability*** *(p)*. The depicted values represent the maximal fEPSP amplitudes after 15 stimulations at 1 Hz (filled squares) and 0.3 Hz (white squares) frequency facilitation. Values have been fitted with a Hill equation. We estimated $p \approx 0.06$ at baseline conditions (0.025 Hz and 1.16 mM Ca_{int}).

Appendix B

Modelling of paired-pulse facilitation

Figure B.1 shows the ratios of paired-pulse facilitation at different interstimulus intervals in dependence of the initial release probability (p at the first pulse; see appendix A for calculation of p). The amount of paired-pulse facilitation decreased with increases in the initial release probability. This points to a direct dependency of the paired-pulse facilitation from the initial release probability. We therefore tested a single sensor model to simulate this dependence. A mathematical description for such kind of dependence is given by Dobrunz and Stevens (1997):

$$Facilitation = 100 \times \frac{1-(1-p)^{\lambda p^{\eta}}}{p} \tag{B.1}$$

The p stands for the initial release probability, η is a factor that depends on the ISIs. λ represents a constant that relies on the intrinsic properties of the specific synapse. We fitted the data sets in figure B.1 (dotted lines) simultaneously yielding $\lambda = 0.75$ and η depending on the ISI (10 ms = -0.23, 40 ms = -0.12, 80 ms = -0.10, and 150 ms = -0.03).

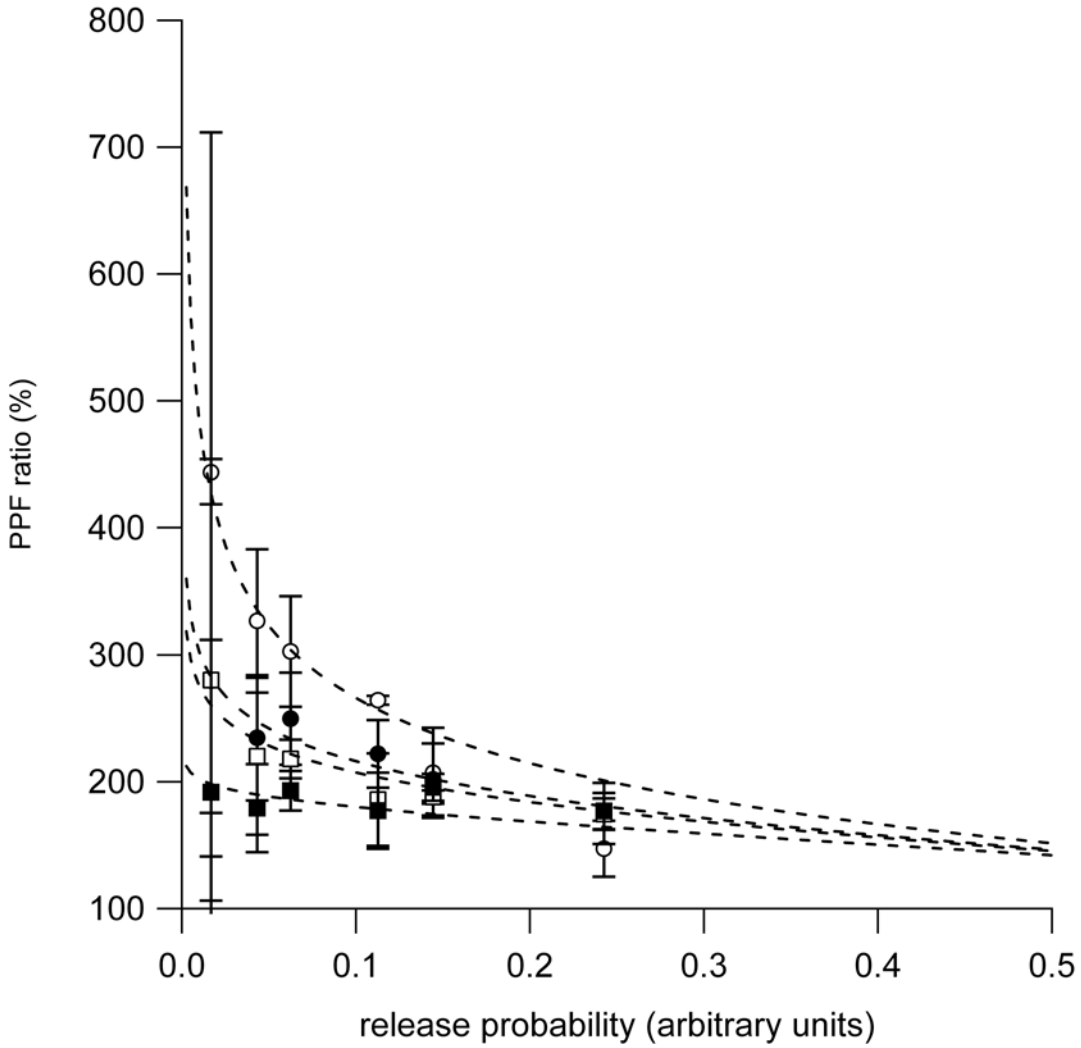

Figure B.1: ***A single site model for paired-pulse facilitation.*** The figure illustrates the ratios of paired-pulse facilitation at different ISIs in dependence of the initial release probability. Superimposed dotted lines represent predications from the single sensor model (see equation B.1).

Appendix C

Parameters of the models

Parameter	non-cooperative	cooperative	cooperative simultaneous
χ^2	17.74	18.74	47.71
Kd_{rel}	2.79	2.69	2.64
n	3.60	3.60	3.60
$coup$	0.57	0.45	0.55
ISI	1.00	1.00	1.00
K_{off}	0.18	0.04	0.14
Kd_{FF}	-0.54*	0.05	0.05
m	n.a.	3.52	4.04
$rf_{0.84}$	0.40	0.36	0.35
$rf_{1.16}$	0.54	0.55	0.49
$rf_{1.35}$	0.48	0.44	0.55
$rf_{1.61}$	0.56	0.63	0.60
$rf_{2.03}$	0.58	0.68	0.67

Figure C.1: ***Fit parameter 1 Hz.*** Overview about the fit parameter calculated by fitting the data sets with the multiple site model for frequency facilitation at 1 Hz. Note that n and ISI where fixed values and have not been determined by the fitting procedure. * In the non-cooperative model best predictions were made using negative values for the parameter Kd_{FF}.

parameter	**non-cooperative**	**cooperative**	**cooperative simultaneous**
χ^2	2.20	4.26	17.47
Kd_{rel}	3.31	2.66	2.64
n	3.60	3.60	3.60
$coup$	0.34	0.45	0.55
ISI	3.30	3.30	3.30
K_{off}	0.06	0.06	0.14
Kd_{FF}	-0.54*	0.11	0.05
m	n.a.	5.71	4.04
$rf_{0.84}$	0.32	0.19	0.35
$rf_{1.16}$	0.53	0.31	0.49
$rf_{1.35}$	0.57	0.35	0.55
$rf_{1.61}$	0.64	0.45	0.60
$rf_{2.03}$	0.62	0.55	0.67

Figure C.2: ***Fit parameter 0.3 Hz.*** Overview about the fit parameter calculated by fitting the data sets with the multiple site model for frequency facilitation at 0.3 Hz. * In the non-cooperative model best predictions were made using negative values for the parameter Kd_{FF}.

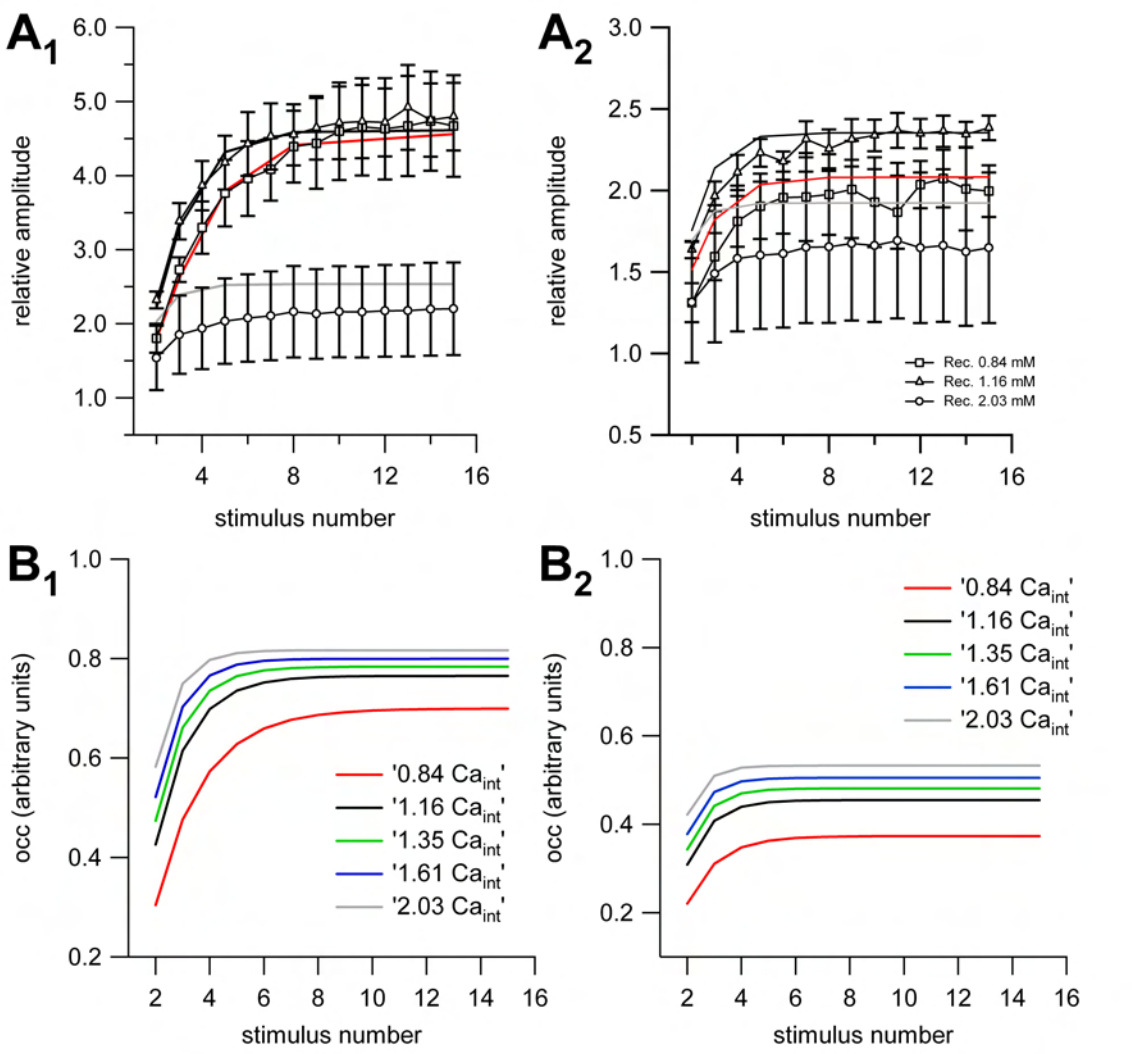

Figure C.3: ***Predictions of the multiple site model.*** $\mathbf{A}_1$ Overlay of MF-fEPSP amplitudes at different Ca_{int} at 1 Hz stimulation frequency and predictions of the model (solid lines). $\mathbf{A}_2$ same as A_1 for 0.3 Hz stimulations. $\mathbf{B}_1$ depicts the occupancy of the Ca^{2+} binding site of the frequency facilitation sensor at different Ca_{int} for 1 Hz. $\mathbf{B}_2$ Same as B_1 for 0.3 Hz.